



## **Interdependency of EGF and GLP-2 Signaling in Attenuating Mucosal Atrophy in a Mouse Model of Parenteral Nutrition**

Feng, Yongjia; Demehri, Farok R; Xiao, Weidong; Tsai, Yu-Hwai; Jones, Jennifer C; Brindley, Constance D; Threadgill, David W; Holst, Jens J; Hartmann, Bolette; Barrett, Terrence A; Teitelbaum, Daniel H; Dempsey, Peter J

*Published in:*  
Cellular and Molecular Gastroenterology and Hepatology

*DOI:*  
[10.1016/j.jcmgh.2016.12.005](https://doi.org/10.1016/j.jcmgh.2016.12.005)

*Publication date:*  
2017

*Document version*  
Publisher's PDF, also known as Version of record

*Document license:*  
[CC BY-NC-ND](#)

*Citation for published version (APA):*  
Feng, Y., Demehri, F. R., Xiao, W., Tsai, Y-H., Jones, J. C., Brindley, C. D., Threadgill, D. W., Holst, J. J., Hartmann, B., Barrett, T. A., Teitelbaum, D. H., & Dempsey, P. J. (2017). Interdependency of EGF and GLP-2 Signaling in Attenuating Mucosal Atrophy in a Mouse Model of Parenteral Nutrition. *Cellular and Molecular Gastroenterology and Hepatology*, 3(3), 447-468. <https://doi.org/10.1016/j.jcmgh.2016.12.005>

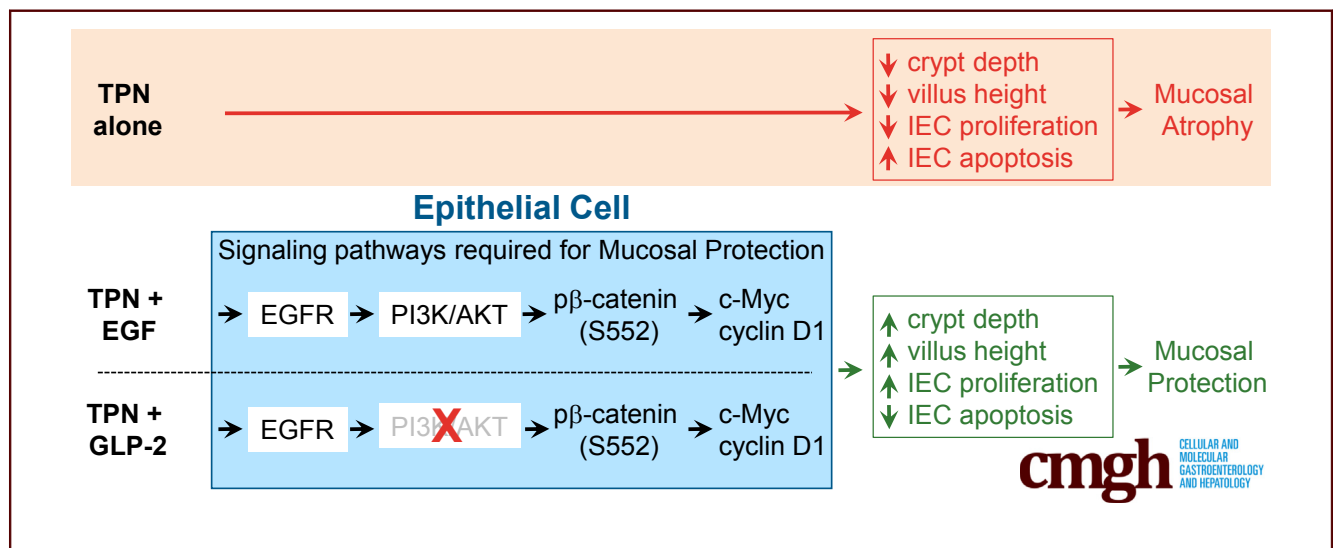
## ORIGINAL RESEARCH

## Interdependency of EGF and GLP-2 Signaling in Attenuating Mucosal Atrophy in a Mouse Model of Parenteral Nutrition



Yongjia Feng,<sup>1</sup> Farok R. Demehri,<sup>1</sup> Weidong Xiao,<sup>1</sup> Yu-Hwai Tsai,<sup>2</sup> Jennifer C. Jones,<sup>3,4</sup> Constance D. Brindley,<sup>3</sup> David W. Threadgill,<sup>5</sup> Jens J. Holst,<sup>6</sup> Bolette Hartmann,<sup>6</sup> Terrence A. Barrett,<sup>7</sup> Daniel H. Teitelbaum,<sup>1,†</sup> and Peter J. Dempsey<sup>3,4</sup>

<sup>1</sup>Section of Pediatric Surgery, Department of Surgery, <sup>2</sup>Division of Gastroenterology, Department of Internal Medicine, University of Michigan Medical School and the C. S. Mott Children's Hospital, Ann Arbor, Michigan; <sup>3</sup>Division of Gastroenterology, Hepatology and Nutrition, Department of Pediatrics, <sup>4</sup>Cell Biology, Stem Cells and Development Graduate Program, University of Colorado Medical School, Aurora, Colorado; <sup>5</sup>Department of Veterinary Pathobiology, College of Veterinary Medicine and Biomedical Sciences, Department of Molecular and Cellular Medicine, College of Medicine, Texas A&M University, College Station, Texas; <sup>6</sup>Novo Nordisk Foundation Center for Basic Metabolic Research and Department of Biomedical Sciences, University of Copenhagen, Panum Institute, Copenhagen, Denmark; <sup>7</sup>Division of Digestive Diseases and Nutrition, Department of Internal Medicine, University of Kentucky, Lexington, Kentucky



## SUMMARY

Enteral nutrient deprivation reduced endogenous epidermal growth factor (EGF) and glucagon-like peptide-2 signaling in mice and human beings. In a mouse model of total parenteral nutrition, both exogenous EGF and glucagon-like peptide-2 required EGF receptors to attenuate mucosal atrophy, however, only EGF required phosphatidylinositol 3-kinase/protein kinase B signaling for this beneficial response.

**BACKGROUND & AIMS:** Total parenteral nutrition (TPN), a crucial treatment for patients who cannot receive enteral nutrition, is associated with mucosal atrophy, barrier dysfunction, and infectious complications. Glucagon-like peptide-2 (GLP-2) and epidermal growth factor (EGF) improve intestinal epithelial cell (IEC) responses and attenuate mucosal atrophy in several TPN models. However, it remains unclear whether these 2 factors use distinct or overlapping signaling pathways to improve IEC responses. We investigated the interaction of

GLP-2 and EGF signaling in a mouse TPN model and in patients deprived of enteral nutrition.

**METHODS:** Adult C57BL/6J, *IEC-Egfr<sup>knock out</sup> (KO)* and *IEC-pik3r1<sup>KO</sup>* mice receiving TPN or enteral nutrition were treated with EGF or GLP-2 alone or in combination with reciprocal receptor inhibitors, GLP-2(3-33) or gefitinib. Jejunum was collected and mucosal atrophy and IEC responses were assessed by histologic, gene, and protein expression analyses. In patients undergoing planned looped ileostomies, fed and unfed ileum was analyzed.

**RESULTS:** Enteral nutrient deprivation reduced endogenous EGF and GLP-2 signaling in mice and human beings. In the mouse TPN model, exogenous EGF or GLP-2 attenuated mucosal atrophy and restored IEC proliferation. The beneficial effects of EGF and GLP-2 were decreased upon Gefitinib treatment and in TPN-treated *IEC-Egfr<sup>KO</sup>* mice, showing epidermal growth factor–receptor dependency for these IEC responses. By contrast, in TPN-treated *IEC-pik3r1<sup>KO</sup>* mice, the beneficial actions of EGF were lost, although GLP-2 still attenuated mucosal atrophy.

**CONCLUSIONS:** Upon enteral nutrient deprivation, exogenous GLP-2 and EGF show strong interdependency for improving IEC responses. Understanding the differential requirements for phosphatidylinositol 3-kinase/phosphoAKT (Ser473) signaling may help improve future therapies to prevent mucosal atrophy. (*Cell Mol Gastroenterol Hepatol* 2017;3:447-468; <http://dx.doi.org/10.1016/j.jcmgh.2016.12.005>)

**Keywords:** Total Parenteral Nutrition; EGF; GLP-2; EGFR; PI3K; Mucosal Atrophy.

Although total parenteral nutrition (TPN) is vital for the nutritional support of patients who cannot tolerate enteral nutrition, TPN is associated with mucosal atrophy and loss of intestinal integrity that can lead to numerous clinical complications, including higher rates of bacterial translocation and septicemia.<sup>1-4</sup> A more detailed understanding of the signaling pathways responsible for TPN-related intestinal complications therefore is needed to improve therapeutic options and clinical outcomes for patients dependent on TPN. Teduglutide, a stable analog of glucagon-like peptide 2 (GLP-2), is one new therapeutic approach that is undergoing extensive clinical trials for the treatment of patients with intestinal failure.<sup>5,6</sup> A recent report showed long-term teduglutide treatment was effective in reducing parenteral support in patients with short-bowel syndrome (SBS),<sup>6</sup> however, the mechanisms underlying the beneficial actions of GLP-2 and its analogs in the gut are complex and still poorly defined.

GLP-2 (1-33) is a 33-amino acid peptide hormone secreted by enteroendocrine L cells in the distal small bowel and proximal colon but its biological actions are primarily in the proximal small intestine.<sup>7</sup> The main stimulus for GLP-2 secretion is the presence of enteral nutrients, such as fats and carbohydrates. However, because GLP-2 receptors (GLP2Rs) are expressed only in enteric neurons, enteroendocrine cells, and subepithelial myofibroblasts, the majority of GLP-2 actions on the mucosal epithelium occur indirectly through paracrine mediators. The trophic actions of GLP-2 on crypt cell proliferation occur through complex signaling events involving several paracrine factors, including insulin-like growth factors (IGFs), epidermal growth factor (EGF), and other erythroblastic leukemia viral oncogene homolog (ErbB) ligands and keratinocyte growth factors that are produced by nonepithelial cells that act in a region-specific and context-dependent manner.<sup>8-10</sup>

Two of the most well-studied models of GLP-2 action are mucosal growth in response to exogenous GLP-2 administration and endogenous GLP-2 signaling required for adaptive mucosal responses after refeeding.<sup>8,9</sup> Previous studies using *Igf1*-deficient mice and intestinal epithelial cell (IEC)-specific IGF-1 receptor-deficient mice have proposed that IGF-1 produced by subepithelial myofibroblasts is required for the intestinotrophic actions of GLP-2, and both exogenous GLP-2 and IGF-I can activate several growth-related signaling pathways including  $\beta$ -catenin, protein kinase B (AKT), and c-Myc.<sup>11-14</sup> However, GLP-2 can still

induce AKT activation in IGF-1-deficient mice,<sup>11,14</sup> suggesting that other growth factors contribute to the beneficial actions of GLP-2 in the intestine. For example, exogenous GLP-2, but not IGF-I, was shown to selectively activate ErbB ligand expression and this response was lost in *Glp2r*-deficient mice. Moreover, the induction of ErbB ligand expression and enhanced crypt cell proliferation mediated by exogenous GLP-2 was completely blocked by a pan-ErbB inhibitor, showing that these GLP-2 responses were ErbB dependent.<sup>15</sup> Similarly, the same pan-ErbB inhibitor blocked the adaptive growth response to refeeding in wild-type (WT) mice. Refeeding failed to stimulate crypt cell proliferation in *Glp2r*-deficient mice, however, exogenous EGF, but not IGF-1, could restore this trophic response, which was associated with increased AKT phosphorylation.<sup>16</sup> By contrast, the Holst laboratory reported that GLP-2 counteracted intestinal atrophy associated with high-dose EGF-receptor (EGFR)-inhibitor treatment, suggesting an alternative finding that GLP-2 may act independently of an intact EGFR signaling pathway.<sup>17</sup> Overall, these results illustrate the complex nature of GLP-2's actions in intestine and show that several different paracrine signals are involved in GLP-2-dependent signal transduction and mucosal growth responses in vivo. However, the mechanisms regulating these different paracrine signals and the potential for interdependency between their downstream signaling transduction pathways have not been defined.

The mouse TPN model is a valuable experimental approach to study signal transduction pathways contributing to mucosal atrophy in the absence of acute inflammatory changes or small-bowel resection. The removal of enteral nutrition is associated with decreased crypt proliferation, increased IEC apoptosis, a loss of epithelial barrier function, and altered enteric microbiota, resulting in a mild proinflammatory state and mucosal atrophy.<sup>4</sup> We previously showed that tumor necrosis factor (TNF) $\alpha$ /TNF $\alpha$ -receptor 1-mediated down-regulation of functional EGFR signaling in IECs leads to a significant decrease in IEC proliferation and increased IEC apoptosis, and is a major contributor to TPN-associated mucosal atrophy. Importantly, exogenous EGF is able to attenuate mucosal atrophy by maintaining crypt cell proliferation, a beneficial response that is correlated with

#### †Deceased.

**Abbreviations used in this paper:** bp, base pair; EGF, epidermal growth factor; EGFR, epidermal growth factor receptor; GLP-2, glucagon-like peptide 2; GLP2R, glucagon-like peptide 2 receptor; GLP-2 (3-33), glucagon-like peptide 2 antagonist; IEC, intestinal epithelial cell; IGF-1, insulin-like growth factor 1; ISC, intestinal stem cell; IV, intravenous; KO, knock out; Lgr5, leucine-rich repeat-containing G-protein-coupled receptor 5; mRNA, messenger RNA; PCNA, proliferating cell nuclear antigen; PCR, polymerase chain reaction; PI3K, phosphatidylinositol 3-kinase; PI3KR1, phosphatidylinositol 3-kinase p85a; SBS, short-bowel syndrome; TNF, tumor necrosis factor; TPN, total parenteral nutrition; TUNEL, terminal deoxynucleotidyl transferase-mediated deoxyuridine triphosphate nick-end labeling; WT, wild-type.

#### Most current article

© 2017 The Authors. Published by Elsevier Inc. on behalf of the AGA Institute. This is an open access article under the CC BY-NC-ND license (<http://creativecommons.org/licenses/by-nc-nd/4.0/>).

2352-345X

<http://dx.doi.org/10.1016/j.jcmgh.2016.12.005>

restoration of EGFR signaling and partial recovery of AKT phosphorylation.<sup>18–21</sup>

In several different animal TPN models, including the mouse TPN model, exogenous GLP-2 also can improve IEC responses and attenuate mucosal atrophy, further showing that both EGF and GLP-2 are important trophic factors that share many overlapping biological actions in this model.<sup>22–28</sup> In the present study, we examined the interdependency of EGF and GLP-2 and downstream signaling pathways in the mouse TPN model and report several findings. First, we showed that endogenous GLP-2 and EGF signaling is diminished in the mouse TPN model. Second, exogenous EGF and GLP-2 treatments attenuated TPN-induced mucosal atrophy. When the same growth factor treatments were combined with reciprocal inhibitor studies using GLP-2 (3–33) and gefitinib, respectively, we found a strong interdependency of EGF and GLP-2 signaling pathways in preventing the TPN-associated decrease in IEC proliferation and increase in IEC apoptosis. By using intestinal cell-specific *Egfr*-deficient and intestinal cell-specific phosphatidylinositol 3-kinase p85a (*pi3kr1*)-deficient mice, we further showed that both factors require functional EGFR signaling in IECs for their beneficial actions. However, the requirements for functional phosphatidylinositol 3-kinase (PI3K)/phosphoAKT (Ser473) (pAKT) signaling in IECs are divergent. Exogenous EGF is completely dependent on PI3K/pAKT signaling within IECs, whereas GLP-2 is only partially dependent on this pathway and appears to modulate IEC proliferation via Wnt/ $\beta$ -catenin signaling. Finally, analysis of paired human samples of distal small bowel from fed and unfed individuals showed that nutrient deprivation reduced EGF, EGFR, and proglucagon messenger RNA (mRNA) levels and was associated with reduced proliferation and increased apoptotic marker expression. Overall, these findings show important and unique interactions between EGF and GLP-2 that may help guide future therapies to prevent mucosal atrophy, and potentially augment the treatment of disorders such as SBS.

## Materials and Methods

### Mice

C57BL/6J (Jackson Laboratory, Bar Harbor, ME) were used in this study. *Villin-Cre*, *Egfr*<sup>tm1Dwt</sup> (termed *Egfr*<sup>fllox</sup>), *Ah-Cre*, and *Pik3r1*<sup>tm1Lca</sup> (termed *pik3r1*<sup>fllox</sup>) mouse strains on a C57BL/6J background have been described elsewhere.<sup>29–33</sup> *Villin-Cre* and *Egfr*<sup>fllox/fllox</sup> mice were interbred to generate intestine-specific *Egfr*-knockout mice (*Villin-Cre*;*Egfr*<sup>fllox/fllox</sup>; termed *IEC-Egfr*<sup>knock out [KO]</sup>) and genotype control *Egfr*<sup>fllox/fllox</sup> mice. Recombination and loss of EGFR expression in isolated crypts from adult *IEC-Egfr*<sup>KO</sup> mice was assessed at the genomic DNA and mRNA level. DNA samples from isolated colonic crypts were genotyped for *Egfr*<sup>fllox</sup> (also called *Egfr*<sup>f</sup>), recombined *Egfr* $\Delta$ , and *Villin-Cre* alleles by polymerase chain reaction (PCR). Conditions were 35 cycles (30 s at 94°C, 1 min at 60°C, and 1 min at 72°C) with Taq DNA polymerase (Qiagen, Valencia, CA). The *Egfr*<sup>f</sup> primers were lox3-forward: 5'-GGAGGAAAAGAAAGTCTGCC -3' and lox3-reverse:

5'-CCCATAGTTGGATAGGATGG-3'. The *Vil-Cre* allele primers were CRE-forward: 5'-ACCTGAAGATGTTCCGCGATTATCT-3' and lox3-reverse: 5'-ACCGTCAGTACGTGAGATATCTT-3'. A 348-base pair (bp) PCR product was generated from the *Egfr*<sup>f</sup> allele and a 320-bp PCR product from the wild-type allele (not shown). An approximately 350-bp PCR product was generated from the *Vil-Cre* allele. Cre-recombined *Egfr* allele was detected by PCR using 40 cycles (30 s at 94°C, 20 s at 60°C, and 20 s at 72°C) with primers delta-3 5'-CTCAGC-CAGATGATGTTGAC-3' and Delta-4 5'-CCTCGTCTGTGGAA-GAATA-3'. A 129-bp PCR fragment was amplified from the recombined *Egfr* allele. For analysis of *Egfr* mRNA expression, total RNA was extracted from isolated colonic crypts using TRIzol reagent (Invitrogen, Carlsbad, CA) according to the manufacturer's instructions. One microgram of RNA was used as a template for synthesis of complementary DNA using random primers (Gibco-BRL, Carlsbad, CA) and SuperScript III RT (Life Technologies, Grand Island, NY) in a total reaction volume of 20  $\mu$ L. The Cre-recombined *Egfr* $\Delta$  allele has *Egfr* exon 3 deleted. Real-time PCR was performed using 2 sets of primers anchored within exon 3 using the flanking exons, exon 2 (exons 2–3) or exon 4 (exons 3–4). The complementary DNA was used as a template for PCR amplification of exons 2–3 and exons 3–4, respectively. For exons 2–3, 35 cycles (30 s at 94°C, 1 min at 60°C, and 1 min at 72°C) with primers exon 2 forward: 5'-ATGAAAACACCTATGCCTTAGCC-3', and exon 3 reverse: 5'-TAAGTTCGCGATGGGCAGTTC-3'. The predicted wild-type band was 83 bp. For exons 3–4, 35 cycles (30 s at 98°C, 1 min at 60°C, and 1 min at 72°C) with primers exon 3 forward: 5'-CCCATGCGGAACCTACAGGAA-3' and exon 4 reverse: 5'-TTGGATCACATTTGGGGCAAC-3'. The predicted wild-type band was 172 bp.

*Ah-Cre* and *pik3r1*<sup>fllox/fllox</sup> mice were interbred to generate conditional *Pik3r1*-knockout mice (*Ah-Cre*;*pik3r1*<sup>fllox/fllox</sup>; termed *IEC-pik3r1*<sup>KO</sup> mice). In *IEC-pik3r1*<sup>KO</sup> mice, Cre recombinase was induced by intraperitoneal injection of 80 mg/kg of  $\beta$ -naphthoflavone (Sigma, St. Louis, MO) dissolved in corn oil (8 mg/mL; Sigma) during the 6 days before TPN administration. Upon Cre recombinase expression, a specific deletion of active PI3K was observed within the small and large intestinal epithelium owing to a loss of p85 $\alpha$ , p55 $\alpha$ , and p50 $\alpha$  subunits as previously described.<sup>31</sup> All mice were maintained under specific pathogen-free conditions in a controlled temperature, humidity, and light environment. All experimental procedures were conducted in accordance with the University Committee on Use and Care of Animals at the University of Michigan (no. 03986) and University of Colorado (B102614 (01)1E).

### Parenteral Nutrition Animal Model

Sex- and age-matched (10–12 weeks of age) mice initially were fed ad libitum with standard mouse chow and water, and allowed to acclimate for 1 week before surgery. During the administration of intravenous (IV) solutions, mice were housed in metabolic cages to prevent coprophagia. Catheterized mice initially received 5% dextrose in 0.45 N saline, with 20 mEq of KCl/L at 4.8 mL/day as described previously.<sup>19,21</sup> After 24 hours, mice were

randomized to enteral fed control or TPN groups. Enteral controls received intravenous solution at 0.2 mL/h and standard laboratory chow. TPN mice received IV TPN solution at 4.8 mL/day. Nitrogen and energy delivery were matched between groups (isonitrogenous/isocaloric). Mice were killed 7 days after cannulation using CO<sub>2</sub>.

For exogenous growth factor studies, mice received recombinant human EGF (50 µg/kg/day; Sigma-Aldrich, St. Louis, MO) by oral gavage twice daily or human GLP-2 (1-33) (termed GLP-2) (100 µg/kg/day; CA Peptide Research, Napa, CA) subcutaneously by Alzet minipump

(Durect Corp, Cupertino, CA). In both cases, growth factor administration was started after day 1 of TPN and continued until mice were killed as outlined in Figure 1.<sup>10,17,19,34</sup>

For EGFR kinase inhibitor studies, mice received gefitinib (2.5 mg/mL in 1% aqueous Tween 80, 200 µL; LC Laboratories, Woburn, MA) by oral gavage twice daily, starting 3 days before IV cannulation and continued until mice were killed.<sup>19,21</sup> In previous TPN studies, we have shown that gefitinib does not alter crypt cell proliferation or crypt depth in sham-treated control mice.<sup>19</sup> Gefitinib is a

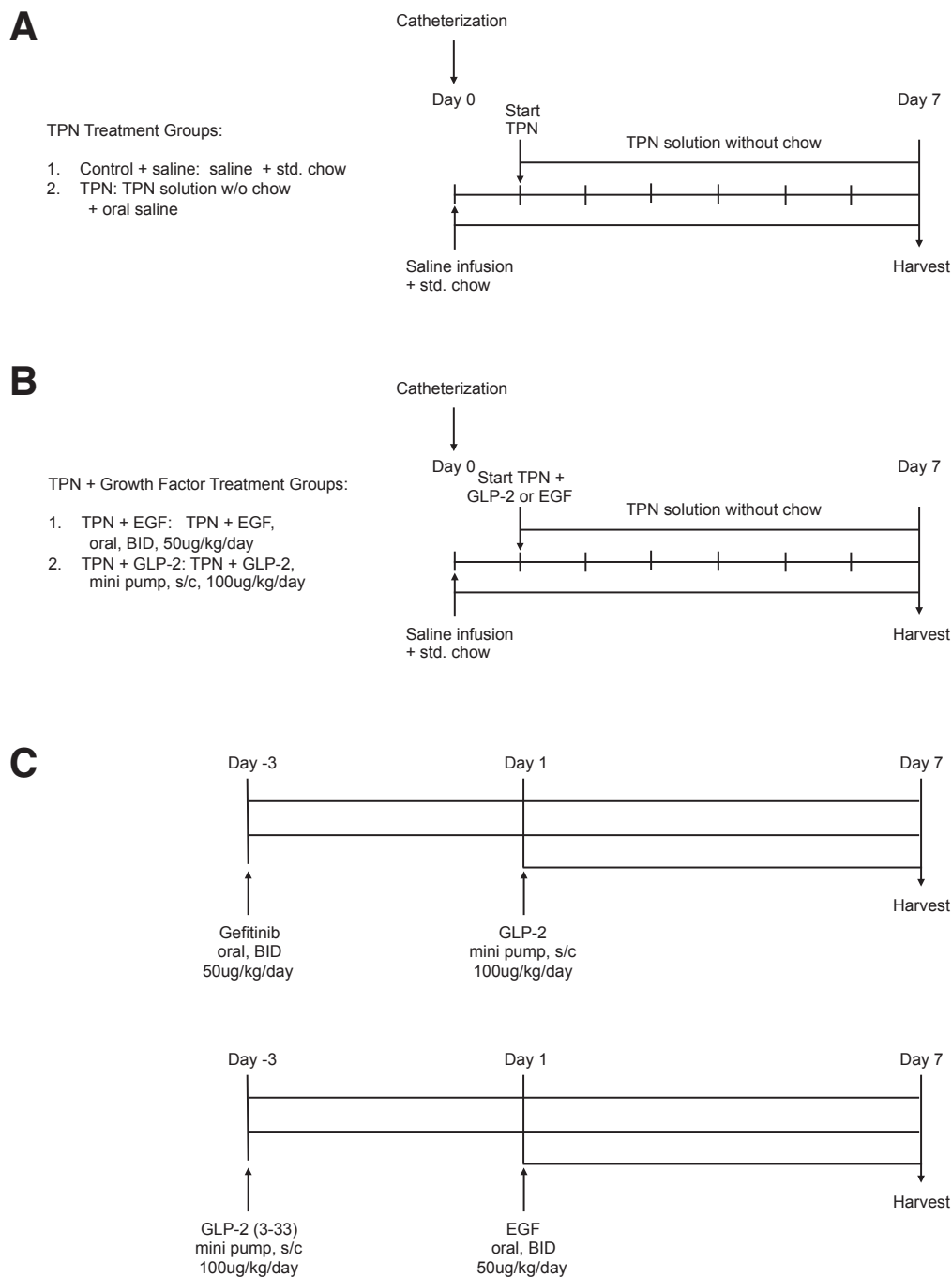


**Figure 1. Schematic outline of mouse TPN model and different growth factor and receptor inhibition experiments performed in this study.** (A) Standard TPN mouse model. (B) TPN and exogenous GLP-2 and EGF treatment regimens. (C) TPN and growth factor treatment regimens combined with reciprocal receptor inhibition. *Upper panel:* TPN + GLP-2 + EGFR kinase inhibitor gefitinib. *Lower panel:* TPN + EGF + GLP-2 antagonist, GLP-2 (3-33). bid, twice daily; s/c, subcutaneously; std, standard.



specific inhibitor for EGFR and does not cross-react with other ErbB receptors.<sup>35</sup> For GLP-2-inhibitor studies, mice received GLP-2-receptor antagonist GLP-2 (3-33) (100 µg/kg/day; CA Peptide Research) subcutaneously by Alzet minipump, starting 3 days before IV cannulation and continued until mice were killed.<sup>36,37</sup> In some experiments, treatment combinations of EGF with GLP-2 (3-33) and GLP-2 with gefitinib were used as outlined in Figure 1. Control mice received a vehicle solution.

### Real-Time PCR

Freshly isolated mouse jejunal crypts or mucosal scrapings were placed immediately into TRIzol (Invitrogen, Carlsbad, CA) and RNA extraction was processed as described previously.<sup>18,19</sup> Quantitative reverse-transcription PCR was performed with SYBR Green dye (ThermoFisher Scientific, Carlsbad, CA) using mouse primers as previously described<sup>18,19</sup> or using human primers listed in Table 1. Expression levels were determined with triplicate assays per sample and normalized to the expression of 18S ribosomal RNA.

### Western Blotting

IECs were isolated from the jejunum, protein extracts were prepared, and then immunoblotting was performed as described previously.<sup>19,38</sup> Protein levels were expressed as a ratio to glyceraldehyde-3-phosphate dehydrogenase protein levels except for analysis of Egfr recombination in IECs of IEC-EgfrKO mice, in which β-actin was used as a loading control. In some experiments, IECs were separated further into nuclear and cytosolic fractions for immunoblotting as described previously.<sup>39,40</sup> For cytoplasmic extracts, protein levels were expressed as a ratio to glyceraldehyde-3-phosphate dehydrogenase protein levels, whereas for nuclear extracts, protein levels were expressed as a ratio to histone H3 protein levels. Western blotting was performed using primary antibodies outlined in Table 2. Secondary antibodies were the corresponding horseradish-peroxidase-conjugated goat anti-mouse antibody or goat anti-rabbit antibodies (Santa Cruz Biotechnology, Santa Cruz, CA).

### Immunohistochemistry and Immunofluorescence

Zinc-formalin fixed (10%) and paraffin-embedded tissue sections and 4% paraformaldehyde-fixed frozen tissue sections of jejunum were stained using standard immunostaining procedures as described previously.<sup>19,21</sup> Immunostaining was performed using primary antibodies outlined in Table 2.

### Intestinal Morphology Assessment

Small intestinal length from the pyloric sphincter to the ileocecal sphincter was measured. Villus height and crypt depth were measured in at least 10 well-oriented, full-length crypt-villus units per specimen and averaged as described previously.<sup>21</sup>

**Table 1. Primer List**

Gene	Sequence
<i>h-GCG-F (proglucagon)</i>	GCAGACCCACTCAGTGATCC
<i>h-GCG-R (proglucagon)</i>	GAATGTGCCCTGTGAATGGC
<i>h-GLP2R-F</i>	GAATGTGCCCTGTGAATGGC
<i>h-GLP2R-R</i>	CTGAGCTCTCTTCACTCCACC
<i>h-EGF-F</i>	CTTGGGAGCCTGAGCAGAAA
<i>h-EGF-R</i>	GCTGCTGCAGTTTCCTTTCC
<i>h-EGFR-F</i>	CCTGGTCTGGAAGTACGCAG
<i>h-EGFR-R</i>	GCGATGGACGGGATCTTAGG
<i>h-PCNA-F</i>	CAGAGCTCTTCCCTTACGCA
<i>h-PCNA-R</i>	GTCCTTGAGTGCCTCCAACA
<i>h-BCL2-F</i>	GGTGAAGTGGGGGAGGATTG
<i>h-BCL2-R</i>	GCCCAGACTCACATCACCAA
<i>h-BCLXL-F (BCL21)</i>	GAAGTGGGGGAGGATTGTGG
<i>h-BCLXL-R (BCL21)</i>	CCGTACAGTTCACAAAGGC
<i>h-ACTB-F</i>	GTCATTCCAAATATGAGATGCGT
<i>h-ACTB-R</i>	GCTATCACCTCCCCTGTGTG
<i>m-Egf-F</i>	TTCTCACAAGGAAAGAGCATCTC
<i>m-Egf-R</i>	GTCCTGTCCCGTTAAGGAAAC
<i>m-Egfr-F</i>	GCATCATGGGAGAGAACAACA
<i>m-Egfr-R</i>	TCAGGAACCACTACTCCATAGGT
<i>m-Glp2r-F</i>	GGAGACAGTTCAGAAGTGGGC
<i>m-Glp2r-R</i>	GCCAGCACACGTACTTATCAA
<i>m-Igf1-F</i>	CTGGACCAGAGACCCCTTTGC
<i>m-Igf1-R</i>	GGACGGGGACTTCTGAGTCTT
<i>m-Igf1r-F</i>	GTGGGGGGCTCGTGTTCCTC
<i>m-Igf1r-R</i>	GATCACCGTGCAGTTTCCA
<i>m-Actb-F</i>	ATGGAGCCGGACAGAAAAGC
<i>m-Actb-R</i>	CTTGCCACTCAGGGAAGGA
<i>18S rRNA-F</i>	GTAACCCGTTGAACCCATT
<i>18S rRNA-R</i>	CCATCCAATCGGTAGTAGCG

GCG, proglucagon; Igf1r, insulin-like growth factor 1 receptor; rRNA, ribosomal RNA.

### IEC Proliferation and Apoptosis Measurements

For IEC proliferation, immunofluorescent staining of proliferating cell nuclear antigen (PCNA) was performed as described previously.<sup>19</sup> The total number of proliferating cells per crypt was defined as the mean of proliferating cells in 10 crypts for each mouse. The results are expressed as a Proliferation Index (the number of PCNA-positive cells per crypt) and then converted to percentage of controls (control values set at 100%). PCNA protein and mRNA levels in cell extracts also were expressed relative to controls. Terminal deoxynucleotidyl transferase-mediated deoxyuridine triphosphate nick-end labeling (TUNEL) assay was performed following the manufacturer's instructions (R&D Systems, Minneapolis, MN). Immunofluorescent staining for cleaved caspase-3 was performed to assess IEC apoptosis as described previously.<sup>19</sup> The results are expressed as an Apoptotic Index (the percentage of active caspase-3-positive cells/villi using a mean of 10 villi per mouse) as described previously.<sup>19</sup>

**Table 2.**Antibody List

Antibody	Source	Application/ dilution
Phospho-AKT (S473)	Cell Signaling, Danvers, MA	WB, 1:1000
Total AKT	Cell Signaling	WB, 1:1000
Phospho-β-catenin (S552)	Cell Signaling	WB, 1:500
Phospho-β-catenin (S33/37/T41)	Cell Signaling	WB, 1:500
Total β-catenin	Cell Signaling	WB, 1:1000
Cleaved caspase 3	Cell Signaling	IF, 1:50
Chromogranin A	Santa Cruz Biotechnology	IF, 1:200
Cyclin D1	Cell Signaling	WB, 1:500
EGFR	Santa Cruz Biotechnology	WB, 1:1000
GAPDH	Santa Cruz Biotechnology	WB, 1:500
Phospho-GSK3β (S9)	Cell Signaling	WB, 1:500
Total GSK3 β	Cell Signaling	WB, 1:1000
Histone H3	Santa Cruz Biotechnology	WB, 1:500
PCNA	Rabbit, Cell Signaling	WB, 1:2000
PCNA	Rabbit monoclonal antibody, Cell Signaling	IF, 1:2000
c-Myc	Cell Signaling	WB, 1:500
β-actin	Cell Signaling	WB, 1:500

GAPDH, glyceraldehyde-3-phosphate dehydrogenase; IF, immunofluorescence; WB, Western blot.

**Plasma GLP-2 Measurements**

Plasma GLP-2 was measured by radioimmunoassay with an N-terminal-specific antiserum that measures only GLP-2 with an intact N-terminus as previously described.<sup>23</sup> Blood was collected into chilled tubes containing EDTA (1 mg/mL), Diprotin A/L (0.1 mmol/L; MP Biomedicals, Aurora, OH), and aprotinin (0.01 mmol/L; Calbiochem, La Jolla, CA) to avoid GLP-2 degradation.

**Human Intestinal Tissue Analysis**

All experiments were performed in accordance with the University of Michigan Hospital Institutional Review Board, Institutional Review Board (HUM00024263). All patients with planned loop ileostomy takedowns were considered. This allowed evaluation of fed and unfed small bowel from the same patient via paired analysis, with the proximal ileostomy being exposed to enteral nutrition and the distal segment isolated from enteric flow. To avoid the inherent differences between jejunum and ileum, all samples were from loop ileostomies of the distal ileum. Patients were fed orally and did not receive parenteral nutrition. Stoma duration was at least 6 weeks for all patients. Patients with Crohn’s disease, necrotizing enterocolitis, and acute ischemia

or perforation were excluded because each of these pathologies may intrinsically change IEC proliferation/apoptosis status independently of nutrient delivery.<sup>41,42</sup> All specimens were taken fresh to the Pathology Department from the Operating Room. Portions of intestine not needed for pathologic evaluation were placed into RPMI 1640 with glutamine (Invitrogen, Carlsbad, CA) for immediate transport to the laboratory on ice. An approximately 1-cm<sup>2</sup> segment of tissue underwent mucosal scraping and was snap-frozen in TRIzol for mRNA analysis. If available, a second segment was placed into optimum cutting temperature embedding compound (PELCO International, Redding, CA), and snap-frozen for subsequent immunofluorescence staining.

**Data Analysis**

Data were expressed as means ± SEM. Statistical analysis used unpaired *t* tests for comparison of 2 means, and a 1-way analysis of variance for comparison of multiple groups (with a Tukey post hoc analysis to assess statistical differences between groups). For analysis of human fed and unfed intestinal samples, a paired *t* test with a nonparametric Wilcoxon matched-pairs signed rank test was used. All statistical analysis was performed using Prism 6 software (GraphPad Software, Inc, San Diego, CA). Statistical significance was defined at a *P* value of less than .05.

**Results**

**Plasma GLP-2 and Mucosal GLP2R Levels Are Reduced in TPN-Treated WT Mice**

GLP2R and EGFR/ErbB pathways are essential components of the signaling network involved in intestinal growth responses and for adaptive mucosal responses to fasting and refeeding.<sup>15,16</sup> In the mouse TPN model, we previously showed that EGFR protein levels in IECs and mucosal *Egf* mRNA levels are reduced markedly in TPN-treated WT mice compared with sham controls (Figure 2A and B).<sup>19</sup> To determine whether components of endogenous GLP-2 signaling also were altered in the TPN model, we examined plasma GLP-2 levels and intestinal GLP-2 receptor (GLP2R) expression in TPN-treated WT and sham control mice. In TPN-treated WT mice, there was a significant 2-fold decrease in plasma GLP-2 levels compared with sham controls (sham: 32.1 ± 9.5 pmol/L vs TPN: 15.7 ± 9.4 pmol/L; *P* < .0001) (Figure 2C). Likewise, mucosal *Glp2r* mRNA levels were decreased significantly in TPN-treated WT mice compared with sham controls (Figure 2D). Thus, similar to decreased functional EGFR signaling detected in the TPN model, these results suggest that endogenous mucosal GLP-2 signaling also is reduced in TPN-treated mice.

**Exogenous EGF Restores Plasma GLP-2 Levels and Mucosal GLP2R Expression Whereas Exogenous GLP-2 Restores Mucosal EGF mRNA Levels in TPN-Treated WT Mice**

Recent studies have shown that treatment with either exogenous EGF or GLP-2 can attenuate mucosal atrophy in TPN-treated WT mice.<sup>19,25</sup> To determine whether these

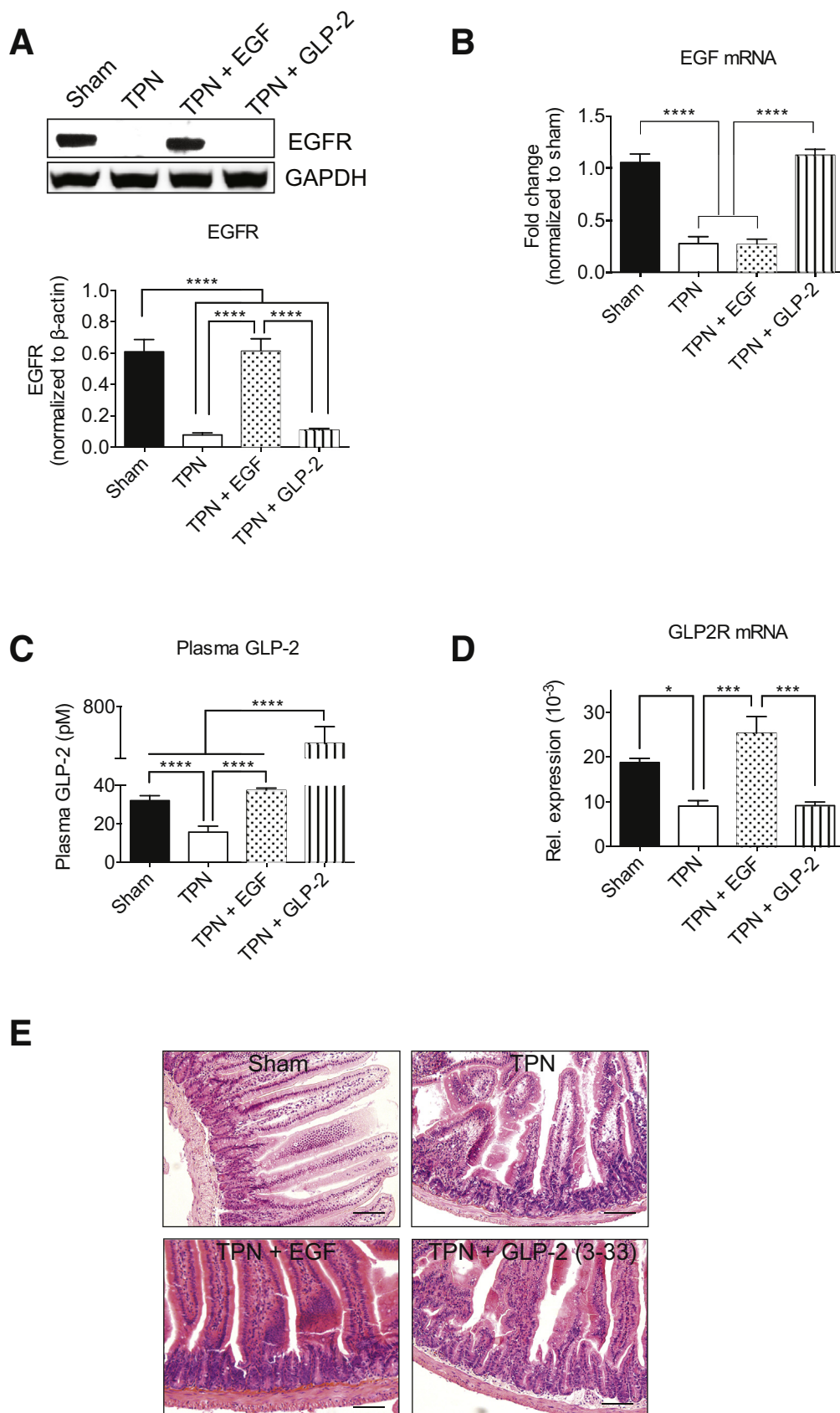


**Figure 2. Exogenous EGF and GLP-2 selectively restore components of their reciprocal signaling pathways in TPN-treated WT mice.** WT mice receiving TPN were treated with exogenous EGF or GLP-2 or vehicle alone. (A) Western blot analysis of EGFR in isolated IECs. *Bottom:* Quantification of EGFR protein levels ( $n = 5$  per group). (B) Real-time PCR analysis of EGF mRNA expression in scraped mucosa ( $n = 6-9$  per group). (C) Radioimmunoassay (RIA) analysis of GLP-2 levels in plasma ( $n = 7-14$  per group). (D) Real-time PCR analysis of GLP2R mRNA expression in scraped mucosa ( $n = 5-7$  per group). (E) H&E analysis. Representative examples of jejunum from sham-treated WT mice and TPN-treated WT mice given vehicle alone, exogenous EGF, or exogenous GLP-2 as described in Figure 1. \* $P < .05$ , \*\*\* $P < .001$ , and \*\*\*\* $P < .0001$ . Scale bars: 50  $\mu$ m. GAPDH, glyceraldehyde-3-phosphate dehydrogenase; Rel, relative.



growth factor treatments altered endogenous EGF and GLP-2 signaling in the TPN model, we examined the same signaling parameters in TPN-treated WT mice given exogenous EGF, GLP-2, or vehicle alone (Figure 1). In agreement with our previous studies,<sup>19</sup> exogenous EGF restored functional EGFR protein levels in IECs of TPN-treated mice (Figure 2A). However, this same EGF treatment failed to restore mucosal *Egf* mRNA expression in TPN-treated mice (Figure 2B). Based on these earlier-described observations, we tested whether exogenous EGF treatment also could affect endogenous GLP-2 signaling in TPN-treated WT mice. Surprisingly, exogenous EGF treatment restored plasma GLP-2 (EGF,  $34.7 \pm 6.6$  pmol/L) levels and mucosal *Glp2r* mRNA expression in TPN-treated WT mice to sham levels (Figure 2C and D). These results suggest that restoration of endogenous GLP-2 signaling may contribute to the actions of exogenous EGF treatment in reducing mucosal atrophy in TPN-treated WT mice.

We next examined the effects of exogenous GLP-2 treatment on the same signaling parameters in the TPN model. As expected, exogenous GLP-2 administration dramatically increased the plasma GLP-2 level more than 200-fold over the sham group ( $657 \pm 172.8$  pmol/L) (Figure 2C). However, exogenous GLP-2 treatment failed to alter mucosal *Glp2r* mRNA levels, which remained at the reduced levels found in TPN-treated WT mice (Figure 2D). Although exogenous GLP-2 did not improve EGFR protein levels in IECs of TPN-treated mice (Figure 2A), the down-regulation of mucosal *Egf* mRNA levels in TPN-treated mice was completely prevented by exogenous GLP-2 treatment (Figure 2B). Thus, exogenous EGF prevents the loss of plasma GLP-2 levels and mucosal *Glp2r* mRNA expression whereas exogenous GLP-2 prevents the loss of mucosal *Egf* mRNA levels in TPN-treated mice. Taken together, these results suggest EGF and GLP-2 signaling pathways interact with each other upon enteral nutrient deprivation.

### **Exogenous GLP-2 and EGF Treatments Attenuate TPN-Induced Mucosal Atrophy**

To further investigate the interdependence of GLP-2 and EGF signaling within the TPN model, we first confirmed that both exogenous growth factor treatments attenuate mucosal atrophy in TPN-treated WT mice.<sup>19,25</sup> H&E analyses of jejunal tissue sections showed that TPN-treated WT mice given vehicle alone had mucosal atrophy with a significant reduction in crypt depth and villus height compared with their sham controls (Figure 2E). By contrast, TPN-treated WT mice given either exogenous GLP-2 or EGF showed protection against mucosal atrophy with significant improvement in both crypt depth and villus height (Figures 2E and 3A and B).

Reduced crypt cell proliferation and increased IEC apoptosis are important features of mucosal atrophy observed in TPN-treated WT mice.<sup>18,19,21</sup> To determine whether exogenous GLP-2 or EGF can maintain crypt cell proliferation in the TPN model, we compared PCNA expression in TPN-treated WT mice administered exogenous GLP-2, EGF, or vehicle alone. In agreement with

previous findings, TPN-treated WT mice given vehicle alone showed a marked reduction in PCNA staining whereas both exogenous GLP-2 and EGF treatments restored crypt cell proliferation to sham control levels (Figure 3C). To test whether the beneficial effects of exogenous GLP-2 and EGF treatments in the TPN model extended to attenuation of IEC apoptosis, we examined TUNEL<sup>+</sup> staining in IECs. As expected, TPN-treated WT mice given vehicle alone had a marked increase in TUNEL<sup>+</sup> staining compared with sham controls whereas TPN-treated WT mice administered exogenous GLP-2 or EGF showed a dramatic reduction in TUNEL<sup>+</sup> staining with apoptotic indexes similar to sham controls (Figure 3D). These results confirm that both exogenous GLP-2 and EGF treatments have significant protective effects against TPN-induced mucosal atrophy that include improvements in crypt depth and villus height, restoration of crypt cell proliferation, and a reduction in IEC apoptosis.

### **Blockade Studies Using EGFR Inhibitor Gefitinib and GLP-2 Antagonist GLP-2 (3-33) Establish a Strong Interdependence of GLP-2 and EGF Signaling Pathways in Reducing Mucosal Atrophy in the TPN Model**

To further elucidate the interconnectivity of exogenous EGF and GLP-2 signaling in attenuating TPN-induced mucosal atrophy, we performed reciprocal inhibitor studies using the EGFR kinase inhibitor gefitinib and the GLP-2 antagonist GLP-2 (3-33). Previous studies have reported that GLP-2 (3-33) can act either as a partial agonist or antagonist for intestinal growth,<sup>34,43</sup> however, the GLP-2 (3-33) dosing regimen used in the current TPN study elicited a weak antagonistic effect on crypt cell proliferation and crypt depth in sham-treated control mice (Figure 4). In WT mice receiving TPN and exogenous GLP-2, gefitinib was given 3 days before administration of TPN and then continued until mice were killed. Conversely, in WT mice receiving TPN and exogenous EGF, GLP-2 (3-33) was given 3 days before administration of TPN and then continued until mice were killed (Figure 1). In both experiments, the opposing inhibitors completely blocked the respective beneficial responses of exogenous GLP-2 and EGF on mucosal atrophy with crypt depth, villus height, and crypt cell proliferation remaining at TPN levels (Figure 3A–D). In addition, both inhibitor treatments significantly increased IEC apoptosis above TPN levels (Figure 3E). The results of these inhibitor studies establish an important interdependent relationship between EGF and GLP-2 signaling pathways in their ability to attenuate mucosal atrophy in the TPN model.

### **Exogenous GLP-2 and EGF Activation of pAkt and Wnt/ $\beta$ -Catenin Signaling in IECs of TPN-Treated Mice Involve Mutually Dependent Signal Transduction Pathways**

In IECs, pAKT and Wnt/ $\beta$ -catenin signaling pathways play critical roles in regulating crypt cell proliferation and

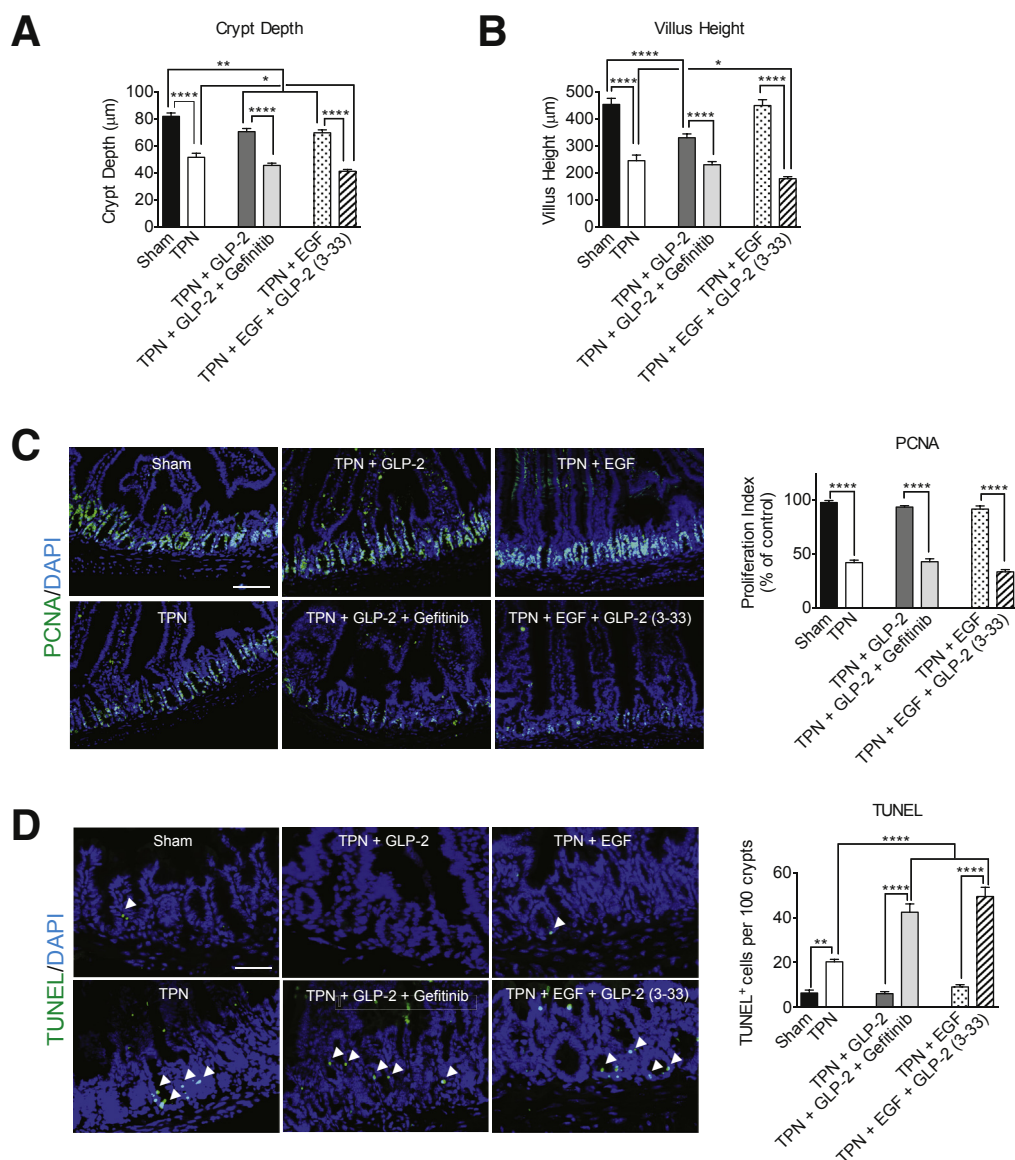


**Figure 3. Reciprocal blockade studies using gefitinib and GLP-2 (3-33) show that exogenous GLP-2 and EGF attenuate TPN-induced mucosal atrophy in an interdependent manner.** (A) Quantification of small intestinal crypt depth ( $n = 16$ – $29$  per group) (B) Quantification of small intestinal villus height ( $n = 8$ – $13$  per group). (C) Immunofluorescent staining of PCNA<sup>+</sup> cells in the jejunum. *Right panel:* Quantification of PCNA<sup>+</sup> cells per crypt expressed as a Proliferation Index ( $n = 5$ – $12$  per group). (D) Immunofluorescent staining of TUNEL<sup>+</sup> cells in the jejunum. *White arrow-heads:* TUNEL<sup>+</sup> cells. Quantification of TUNEL<sup>+</sup> cells per 100 crypts ( $n = 5$  per group). \* $P < .05$ , \*\* $P < .01$ , and \*\*\*\* $P < .0001$ . Scale bars: 50  $\mu$ m. DAPI, 4',6-diamidino-2-phenylindole.

IEC survival. Notably, both exogenous GLP-2 and EGF have been shown to activate pAKT (S473) and Wnt/ $\beta$ -catenin (S552) signaling in several intestinal adaptation and stress models.<sup>12,44–47</sup> To assess changes in the phosphorylation status and total protein levels of AKT,  $\beta$ -catenin, glycogen synthase kinase 3 beta (GSK3 $\beta$ ), and the Wnt target genes cyclin D1 and c-Myc, Western blot was performed from cytoplasmic and nuclear IEC extracts prepared from WT mice receiving TPN. In TPN-treated WT mice, protein levels of pAKT (S473), phospho-GSK3 beta (pGSK3 $\beta$ ) (S9), and total  $\beta$ -catenin were decreased significantly whereas protein levels of phospho-beta-catenin (p- $\beta$ -catenin) (S33/37/T41) were increased dramatically in the cytoplasm (Figure 5A). Importantly, p- $\beta$ -catenin (S552) protein levels in IEC nuclear extracts and the number of p- $\beta$ -catenin (S552)<sup>+</sup>-stained nuclei in crypts were reduced

significantly (Figure 5B and C). These results are consistent with increased GSK3 $\beta$  activity and increased phosphorylation of  $\beta$ -catenin (S33/37/T41), leading to increased proteasomal degradation of  $\beta$ -catenin. The subsequent decrease in nuclear accumulation of p- $\beta$ -catenin (S552) and loss of Wnt transcriptional activity is supported further by the marked reduction in cyclin D1 and c-Myc protein levels in nuclear extracts (Figure 5B–D). Together, these results clearly show that TPN administration significantly reduces pAKT and Wnt/ $\beta$ -catenin signaling within IECs; the dramatic decrease in these 2 signaling pathways is consistent with the loss of crypt cell proliferation and increased IEC apoptosis observed in the TPN-treated WT mice.

By contrast, TPN-treated WT mice given exogenous GLP-2 showed partial restoration of pAKT (S473) and a partial reduction in p- $\beta$ -catenin (S33/37/T41) protein levels,

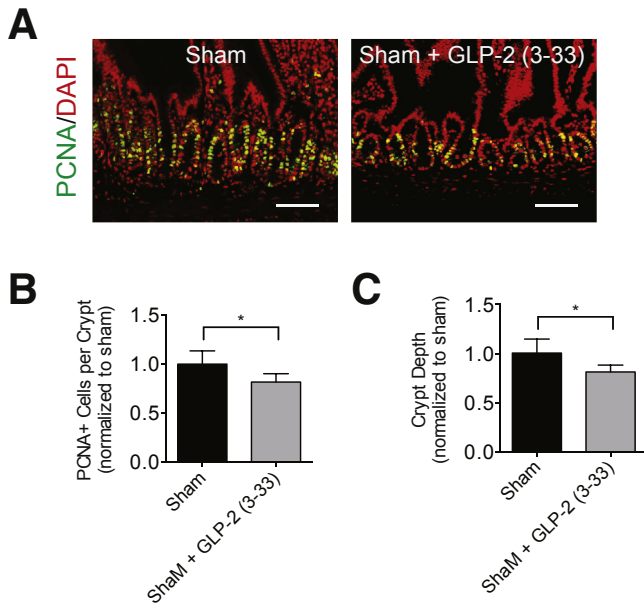


**Figure 4.** GLP-2 (3-33) administered to control mice caused a slight reduction in intestinal growth. Sham-treated control mice received vehicle (phosphate-buffered saline) or GLP-2-receptor antagonist GLP-2 (3-33) (100  $\mu$ g/kg/day) subcutaneously by Alzet minipump, starting 3 days before IV cannulation and continued for another 7 days until mice were killed. (A) Immunofluorescent staining of PCNA<sup>+</sup> cells in the jejunum. (B) Quantification of PCNA<sup>+</sup> cells per crypt. (C) Quantification of small intestinal crypt depth (n = 5 per group). Scale bars: 50  $\mu$ m. \**P* < .05. DAPI, 4',6-diamidino-2-phenylindole.

whereas cytoplasmic pGSK3 $\beta$  (S9) and nuclear p- $\beta$ -catenin (S552) protein levels were completely restored to sham control levels. Consistent with increased pAKT and Wnt/ $\beta$ -catenin signaling and the restoration of cell proliferation in the TPN-treated WT mice given GLP-2, exogenous GLP-2 completely restored cyclin D1 and partially restored c-Myc nuclear protein levels in IECs. Similar increases in pAKT and Wnt/ $\beta$ -catenin signaling were observed with TPN-treated WT mice receiving exogenous EGF. Interestingly, exogenous EGF did not restore pGSK3 protein levels in IECs of TPN-treated mice, suggesting that regulation of GSK3 $\beta$  may be regulated differentially by these 2 growth factors in the TPN model (Figure 5).

Mechanistically, the earlier described results show that exogenous GLP-2 and EGF both attenuate mucosal atrophy in the TPN model, in part by increasing pAKT and Wnt/ $\beta$ -catenin signaling in IECs. To further show that EGF and GLP-2 use the pAKT and Wnt/ $\beta$ -catenin signaling pathways in an interdependent manner, we again used reciprocal inhibitor studies using the EGFR kinase inhibitor gefitinib and the GLP-2 antagonist GLP-2 (3-33) as described earlier. Strikingly, blockade of either EGFR or GLP2R prevented the beneficial effects of the respective growth factors on maintaining pAKT, p- $\beta$ -catenin (S552), cyclin D1, and c-Myc protein levels in the TPN-treated mice (Figure 5). These results clearly show that GLP-2 and EGF both use common downstream signaling

pathways to improve IEC responses in TPN-treated WT mice, and that interconnectivity of GLP2R and EGFR signaling is required for these effects.

### Protective Effect of Exogenous GLP-2 on TPN-Induced Mucosal Atrophy Requires Functional EGFR Signaling in IECs

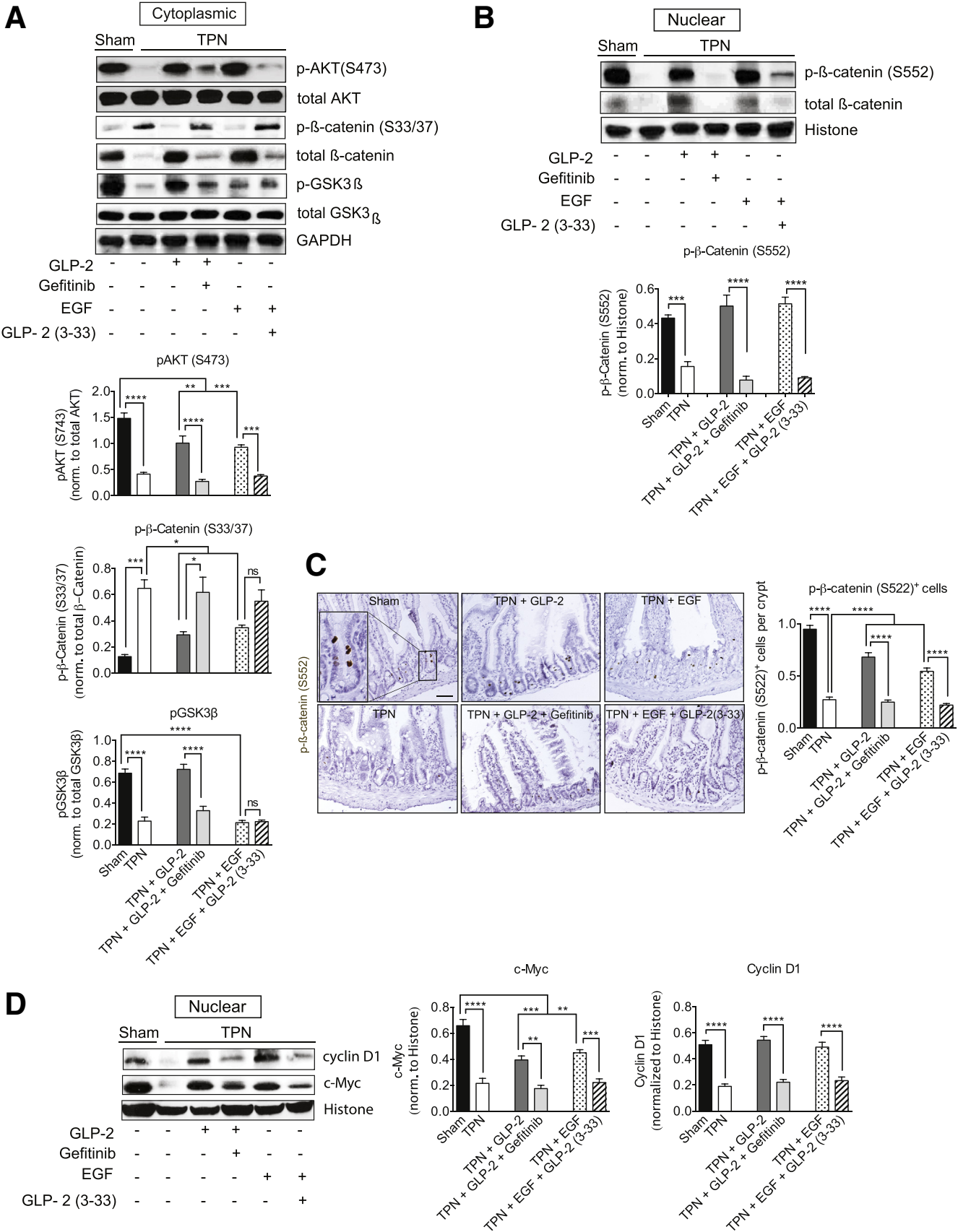
Although GLP2R expression is highest in the jejunum,<sup>48</sup> the lack of GLP2R expression within enterocytes and especially in the intestinal stem/crypt progenitor cells indicates that exogenous GLP-2 mediates its effects on IEC responses via indirect paracrine mechanisms.<sup>8–10,49</sup> To investigate the contribution of EGFR signaling within IECs for the beneficial actions of exogenous GLP-2 in the TPN model, we generated IEC-specific *Egfr*-deficient mice (termed IEC-*Egfr*<sup>KO</sup> mice). Consistent with other reports,<sup>50</sup> these IEC-*Egfr*<sup>KO</sup> mice were healthy and had no overt intestinal phenotype with normal crypt-villus architecture and crypt cell proliferation under normal physiological conditions (Figure 6). Because TPN administration in WT mice completely down-regulates EGFR protein levels in IECs,<sup>19,21</sup> only a direct comparison of IEC responses to exogenous GLP-2 treatment in TPN-treated IEC-*Egfr*<sup>KO</sup> and *Egfr*<sup>fl/fl</sup> genotype control mice was performed.

In TPN-treated genotype control mice, GLP-2 administration continued to prevent mucosal atrophy, but this protective effect was reduced significantly in TPN-treated IEC-*Egfr*<sup>KO</sup> mice and was associated with decreased crypt depth, villus height, and crypt cell proliferation, and a marked increase in IEC apoptosis (Figure 7A–C). Importantly, the protective effect of GLP-2 on p-AKT and Wnt/ $\beta$ -catenin signaling observed in the TPN-treated genotype control mice was diminished significantly in IEC-*Egfr*<sup>KO</sup> mice receiving TPN (Figure 7D–G). Despite GLP-2 not restoring EGFR protein levels in IECs of TPN-treated WT mice (Figure 2), the results from TPN-treated IEC-*Egfr*<sup>KO</sup> mice show that IEC-specific EGFR signaling plays a critical role in how exogenous GLP-2 attenuates TPN-associated mucosal atrophy. In the absence of intestinal EGFRs, the loss of PI3K/AKT and Wnt/ $\beta$ -catenin signaling in IECs suggests that these 2 pathways likely contribute to the beneficial actions of GLP-2 in the mouse TPN model. Because of the lack of conditional GLP2R-deficient mice, it was not possible to perform the reciprocal experiment and test if exogenous EGF required cell type-specific GLP2R signaling to attenuate TPN-induced mucosal atrophy.

### Exogenous GLP-2 Does Not Require Functional PI3K-pAKT Signaling in IECs for its Beneficial Actions on Mucosal Atrophy in the TPN Model

Because exogenous EGF and GLP-2 stimulated pAKT activity in TPN-treated WT mice, we next examined if the beneficial effects of these 2 growth factors were dependent on PI3K-pAKT signaling in IECs. For this analysis, conditional IEC-specific *pi3kr1*<sup>KO</sup> (termed IEC-*pi3kr1*<sup>KO</sup>) mice were used in which the class IA subunit of PI3K was





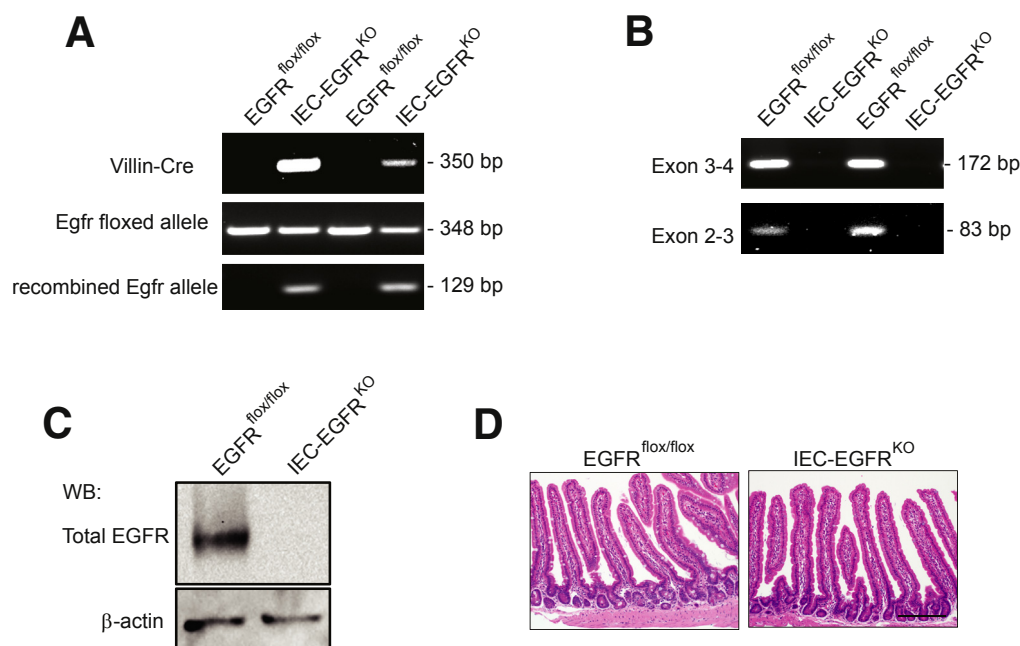


**Figure 6.** *IEC-Egfr<sup>KO</sup>* mice show no overt intestinal phenotype under normal physiological conditions. (A) PCR analysis showing efficient *Egfr* recombination in isolated colonic crypts from *Egfr<sup>flx/flx</sup>* and *IEC-Egfr<sup>KO</sup>* (*Villin-Cre;Egfr<sup>flx/flx</sup>*) mice. (B) Real-time PCR analysis of wild-type *Egfr* mRNA expression in isolated colonic crypts ( $n = 2$  per genotype). Exon 3-anchored primer analysis shows that no wild-type *Egfr* mRNA is detected in colonic epithelium from *IEC-Egfr<sup>KO</sup>* mice. (C) Western blot (WB) analysis of EGFR protein expression in isolated colonic crypts. No EGFR protein is detected in colonic epithelium from *IEC-Egfr<sup>KO</sup>* mice. (D) H&E analysis of the jejunum. No overt changes in crypt-villus architecture are observed in *IEC-Egfr<sup>KO</sup>* mice. Scale bars: 100  $\mu$ m.

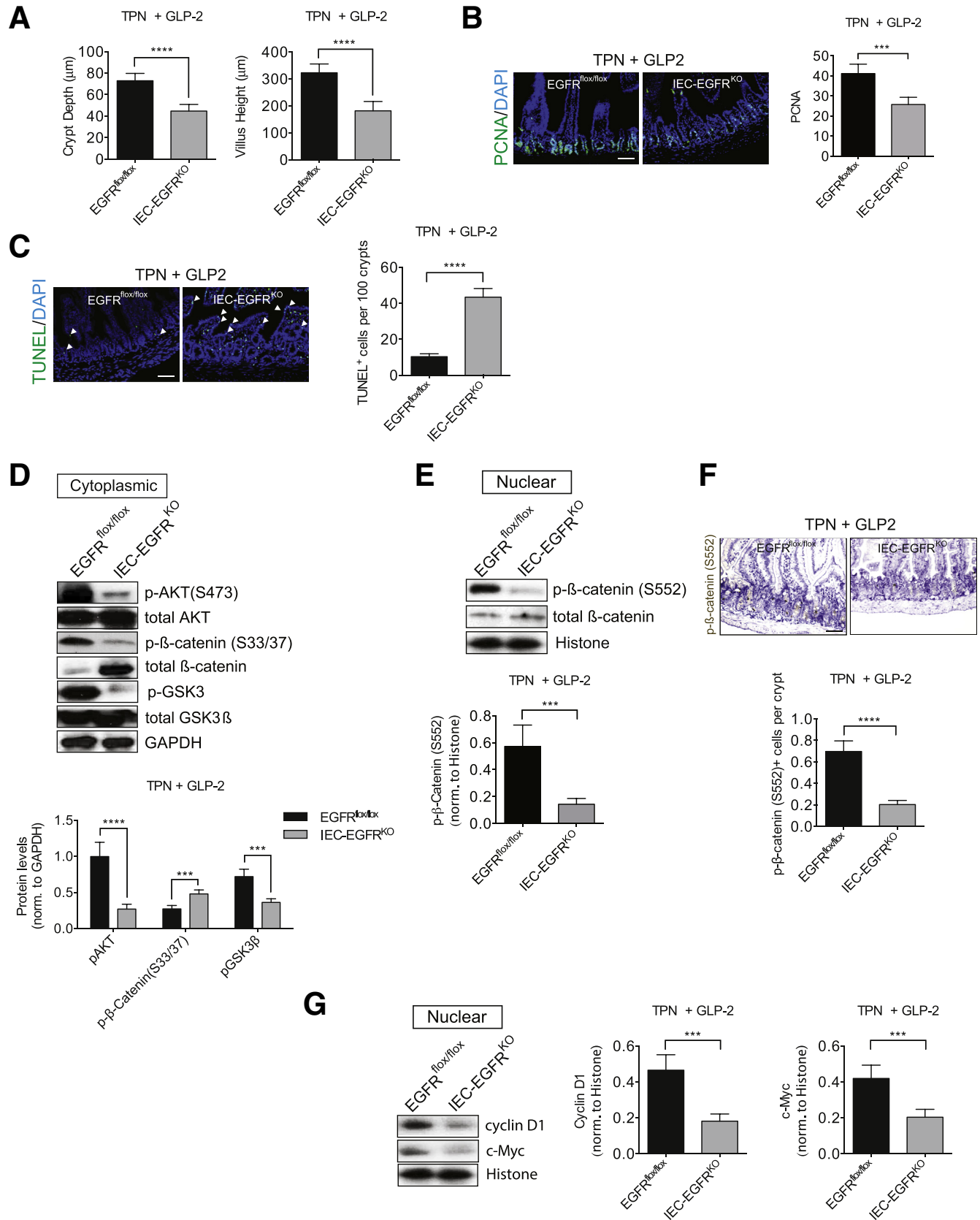
conditionally deleted in IECs.<sup>31</sup> *IEC-pi3kr1<sup>KO</sup>* mice have no intestinal phenotype at baseline<sup>31</sup> but consistent with a loss of functional PI3K activity in IECs, pAKT (S473) levels were reduced dramatically in IECs of *IEC-pi3kr1<sup>KO</sup>* mice under all experimental conditions (Figure 8). Similar to the previous *IEC-Egfr<sup>KO</sup>* studies, only a direct comparison of IEC responses to exogenous growth factor treatments in TPN-treated *IEC-pi3kr1<sup>KO</sup>* and *pi3kr1<sup>fl/fl</sup>* genotype control mice was performed. Surprisingly, exogenous GLP-2 still was able to attenuate mucosal atrophy in TPN-treated *IEC-pi3kr1<sup>KO</sup>* mice. In TPN-treated *IEC-pi3kr1<sup>KO</sup>* mice given GLP-2, crypt depth and villus height were completely restored whereas crypt cell proliferation vastly was improved, although it did not reach the same levels of genotype control mice (Figure 9A–C). Similarly, although crypt IEC apoptosis was increased slightly, it was still greatly diminished compared with the increased apoptosis observed in TPN-treated *IEC-pi3kr1<sup>KO</sup>* mice receiving EGF (see next section) (Figure 9D). Thus, unlike the dramatic loss of protective IEC responses observed in TPN-treated

*IEC-Egfr<sup>KO</sup>* mice receiving GLP-2, exogenous GLP-2 still had significant beneficial effects against mucosal atrophy in the absence of intestinal PI3K-pAKT signaling.

The protective effects of GLP-2 on TPN-treated *IEC-pi3kr1<sup>KO</sup>* mice also were reflected in an overall improvement in Wnt/ $\beta$ -catenin signaling in IECs with both total cytoplasmic  $\beta$ -catenin and nuclear p- $\beta$ -catenin (S552) protein levels being restored completely (Figure 9E and F). Consistent with improved crypt cell proliferation and restoration of Wnt/ $\beta$ -catenin signaling, nuclear cyclin D1 and c-Myc protein levels also were restored to genotype control levels (Figure 9G). These data clearly show that an intact PI3K/pAKT signaling pathway in IECs is not essential for exogenous GLP-2 to protect against loss of crypt cell proliferation and the increase in IEC apoptosis observed in the TPN model. Importantly, the preservation of nuclear  $\beta$ -catenin (S552) with exogenous GLP-2 in TPN-treated *IEC-pi3kr1<sup>KO</sup>* mice suggests that GLP-2 can drive IEC proliferation via an EGFR/Wnt/ $\beta$ -catenin pathway that is regulated independently of intestinal PI3K/pAKT signaling. Although

**Figure 5.** (See previous page). Both exogenous GLP-2 and EGF regulate pAKT and Wnt/ $\beta$ -catenin signaling in IECs to reduce TPN-induced mucosal atrophy. (A) Western blot analysis of pAKT (S473), p- $\beta$ -catenin (S33/37/T41), and pGSK3 $\beta$  in cytoplasmic extracts. Lower panels: Quantification of each phospho-specific protein. pAKT (S473) ( $n = 4$  per group), p- $\beta$ -catenin (S33/37/T41) ( $n = 3$ –5 per group), and pGSK3 $\beta$  ( $n = 4$ –5 per group). (B) Western blot analysis of p- $\beta$ -catenin (S552) in nuclear extracts. Lower panel: Quantification of p- $\beta$ -catenin (S552) protein levels ( $n = 4$ –5 per group). (C) Immunostaining of p- $\beta$ -catenin (S552)<sup>+</sup> cells in the jejunum. Right panel: Quantification of p- $\beta$ -catenin (S552)<sup>+</sup> cells per crypt ( $n = 4$ –5 per group). (D) Western blot analysis of cyclin D1 and c-Myc in nuclear extracts. Right panels: Quantification of nuclear cyclin D1 and c-Myc protein levels ( $n = 4$ –5 per group). \* $P < .05$ , \*\* $P < .01$ , \*\*\* $P < .001$ , and \*\*\*\* $P < .0001$ . Scale bars: 50  $\mu$ m. GAPDH, glyceraldehyde-3-phosphate dehydrogenase; norm, normal.





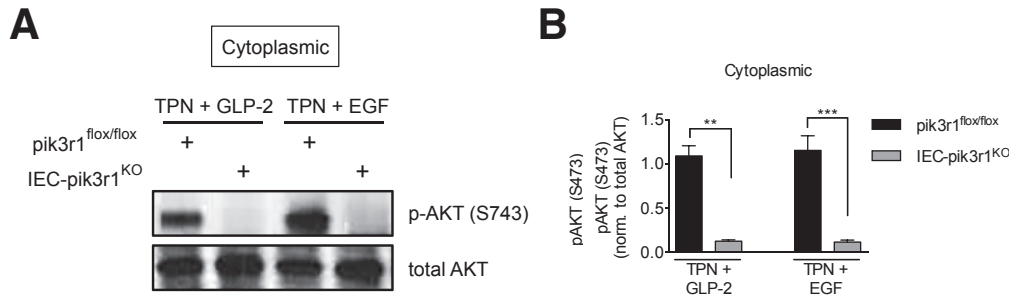


**Figure 8. TPN-treated *IEC-pik3r1<sup>KO</sup>* mice administered exogenous GLP-2 or EGF show a marked loss of functional pAKT signaling in IECs.** (A) Western blot analysis of pAKT (S473) and total AKT protein levels in cytoplasmic extracts from IECs. (B) Quantification of pAKT (S473) protein levels normalized to total AKT protein levels (n = 3 per group). \*\**P* < .01, \*\*\**P* < .001.

not a direct focus of the current study, it will be important to determine whether exogenous GLP-2 can produce similar IEC responses in the absence of PI3K/AKT signaling under normal intestinal homeostasis and during adaptive responses to refeeding.

#### Protective Effect of Exogenous EGF on TPN-Induced Mucosal Atrophy Requires Functional PI3K-pAKT Signaling in IECs

Based on the earlier-described observations with exogenous GLP-2, we next examined whether exogenous EGF required functional PI3K-pAKT signaling in IECs to attenuate TPN-induced mucosal atrophy. As expected, exogenous EGF protected TPN-treated genotype control mice against mucosal atrophy similar to TPN-treated WT mice given EGF. By contrast, exogenous EGF failed to protect against mucosal atrophy in *IEC-pi3kr1<sup>KO</sup>* mice receiving TPN. Indeed, TPN-treated *IEC-pi3kr1<sup>KO</sup>* mice given EGF showed significant reductions in crypt depth, villus height, and crypt cell proliferation, whereas IEC apoptosis was increased dramatically compared with the TPN-treated genotype control mice receiving EGF (Figure 9A–D).

Importantly, isolated IECs from TPN-treated *IEC-pi3kr1<sup>KO</sup>* mice given EGF showed sustained levels of cytoplasmic p-β-catenin (S33/37/T41) whereas nuclear p-β-catenin (S552) levels remained diminished, indicating that EGF could not restore Wnt/β-catenin signaling in IECs in the absence of functional PI3K-AKT signaling (Figure 9E

and F). Furthermore, exogenous EGF failed to restore nuclear cyclin D1 and c-Myc protein levels, providing additional evidence that exogenous EGF was unable to restore Wnt/β-catenin signaling in IECs of TPN-treated *IEC-pi3kr1<sup>KO</sup>* mice (Figure 9G). Together, these results indicate that the beneficial effects of exogenous EGF upon TPN-associated mucosal atrophy require intestinal EGFR/PI3K/pAKT signaling, which plays a critical role for maintaining functional Wnt/β-catenin signaling in IECs of TPN-treated mice.

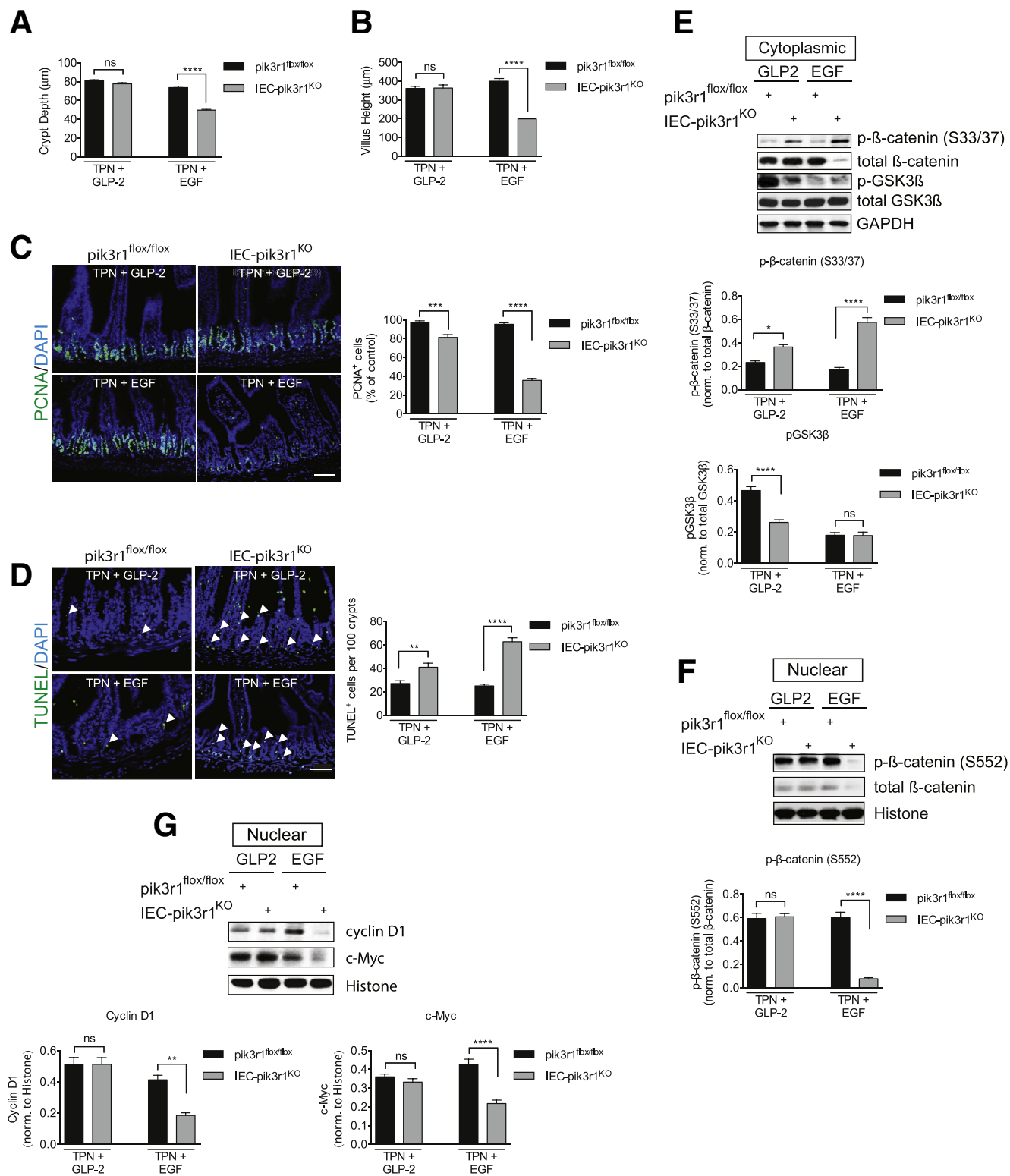
#### GLP-2 and EGF Signaling Are Decreased in Unfed Human Small Intestine

To address whether the reduction in GLP-2 and EGF signaling associated with enteral nutrient deprivation in the mouse also is observed in human beings, paired samples of fed and unfed distal small bowel were collected from patients undergoing planned loop ileostomy take-downs. Although these patients were not on TPN, our laboratory has shown that the adverse effects of TPN are caused by enteral nutrient deprivation and not the mere administration of parenteral nutrition solution.<sup>51</sup> Importantly, the pairing of matched fed and unfed samples from the same patient allowed for direct analysis of any differences in signaling independently of interindividual variation. To assess EGF and GLP-2 signaling in the human samples, *EGF*, *EGFR*, *proglucagon*, and *GLP2R* mRNA expression was measured in fed and unfed ileum obtained from 8 different patients. Interestingly, a significant

**Figure 7. (See previous page). Exogenous GLP-2 does not improve mucosal atrophy in TPN-treated *IEC-Egfr<sup>KO</sup>* mice.** (A) Quantification of small intestinal crypt depth and villus height (n = 7–8 per group). (B) Immunofluorescent staining of PCNA<sup>+</sup> cells in the jejunum. Right panel: Quantification of PCNA<sup>+</sup> cells per crypt expressed as a Proliferation Index. (C) Immunofluorescent staining of TUNEL<sup>+</sup> cells in the jejunum. White arrowheads, TUNEL<sup>+</sup> cells. Right panels: Quantification of TUNEL<sup>+</sup> cells in crypt compartment. (D) Western blot analysis of pAKT (S473), p-β-catenin (S33/37/T41), and pGSK3β in cytoplasmic extracts. Lower panel: Quantification of each phospho-specific protein (n = 3 per group). (E) Western blot analysis of p-β-catenin (S552) in nuclear extracts. Lower panel: Quantification of p-β-catenin (S552) protein levels. (F) Immunostaining of p-β-catenin (S552)<sup>+</sup> cells in the jejunum. Lower panel: Quantification of p-β-catenin (S552)<sup>++</sup> cells per crypt. (G) Western blot analysis of cyclin D1 and c-Myc in nuclear extracts. Right panels: Quantification of nuclear cyclin D1 and c-Myc protein levels. All treatment groups (n = 5) unless specified differently. \*\*\**P* < .001, \*\*\*\**P* < .0001. Scale bars: 50 μm. DAPI, 4',6-diamidino-2-phenylindole; norm, normal.

decrease in *EGF*, *EGFR*, and proglucagon mRNA expression levels was observed in unfed segments compared with matched fed segments. However, no difference in *GLP2R* mRNA expression was detected in the unfed samples

(Figure 10A). Although insufficient tissue was available to perform immunostaining from all 8 patients, PCNA<sup>+</sup> crypt cells were reduced significantly in the unfed compared with matched-fed samples from 5 patients (Figure 10B). In



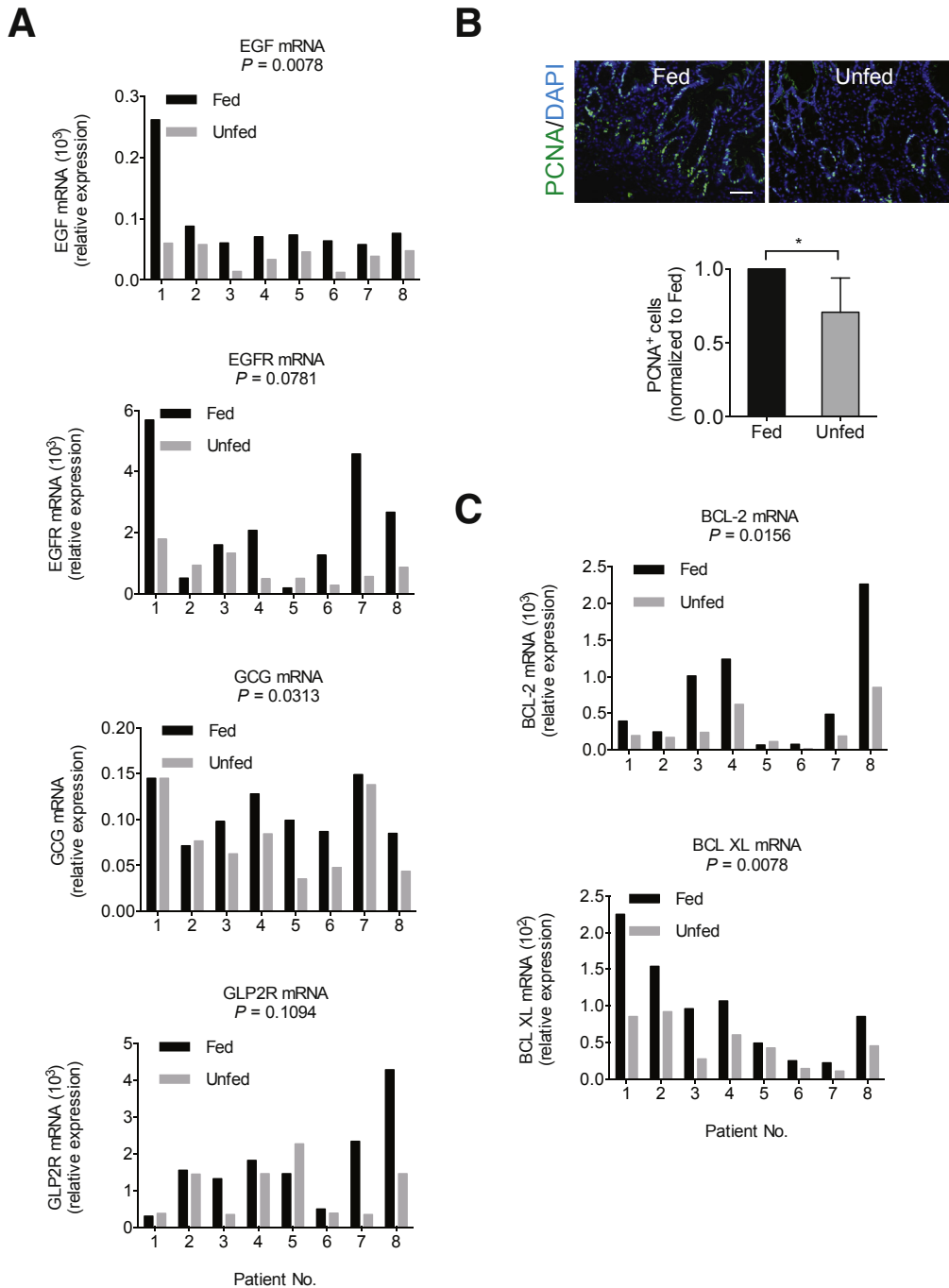


**Figure 10. Reduced GLP-2 and EGF signaling is associated with decreased cell proliferation and increased apoptosis in unfed human small intestine.** Analysis of fed and unfed segments of ileum from patients undergoing planned loop ileostomy take-downs. (A) Real-time PCR analysis of EGF, EGFR, proglucagon (GCG), and GLP2R mRNA expression in scraped mucosa from fed and unfed ileal segments ( $n = 8$ ). (B) Immunofluorescent staining of PCNA. Quantification of PCNA<sup>+</sup> cells per crypt ( $n = 5$ ). (C) Real-time PCR analysis of anti-apoptotic markers BCL-2 and BCL XL mRNA expression in scraped mucosa from fed and unfed ileal segments ( $n = 8$ ). \* $P < .05$ , all other  $P$  values are listed in Figure. DAPI, 4',6-diamidino-2-phenylindole. Scale bars: 50  $\mu$ m.

**Figure 9. (See previous page). Exogenous GLP-2 but not EGF can protect against mucosal atrophy in TPN-treated *IEC-pi3kr1<sup>ko</sup>* mice.** (A) Quantification of small intestinal crypt depth ( $n = 7-8$  per group). (B) Quantification of small intestinal villus height ( $n = 7-8$  per group). (C) Immunofluorescent staining of PCNA<sup>+</sup> cells in the jejunum. Right panel: Quantification of PCNA<sup>+</sup> cells per crypt expressed as a Proliferation Index. (D) Immunofluorescent staining of TUNEL<sup>+</sup> cells in the jejunum. White arrowheads, TUNEL<sup>+</sup> cells. Right panels: Quantification of TUNEL<sup>+</sup> cells in crypt compartment. (E) Western blot analysis of p- $\beta$ -catenin (S33/37/T41) and pGSK3 $\beta$  in cytoplasmic extracts. Lower panels: Quantification of each phospho-specific protein ( $n = 3$  per group). (F) Western blot analysis of p- $\beta$ -catenin (S552) in nuclear extracts. Lower panel: Quantification of p- $\beta$ -catenin (S552) protein levels. (G) Western blot analysis of cyclin D1 and c-Myc in nuclear extracts \* $P < .05$ , \*\* $P < .01$ . Lower panels: Quantification of cyclin D1 and c-Myc protein levels. All treatment groups ( $n = 5$ ) unless specified differently. \*\*\* $P < .001$ , \*\*\*\* $P < .0001$ . Scale bars: 50  $\mu$ m. GAPDH, glyceraldehyde-3-phosphate dehydrogenase; DAPI, 4',6-diamidino-2-phenylindole. \* $P < .05$ , \*\* $P < .01$

addition, in the 1 patient tested, TUNEL+ staining of IECs was increased in the unfed segment compared with the matched-fed sample (data not shown). To further examine if IEC apoptosis was increased in the unfed samples, we measured changes in mRNA expression of the anti-apoptotic factors, BCL-2 and BCL-XL. Significant reductions in *BCL-2* and *BCL-XL* mRNA levels were observed in the unfed segments of ileum compared with the fed control samples from all 8 patients (Figure 10C). Thus, similar to enteral nutrient deprivation in the mouse TPN model, these results indicate that both EGF and GLP-2 signaling pathways are reduced and likely contribute to the reduction in crypt cell proliferation and increased IEC apoptosis observed upon enteral nutrient deprivation in the human ileum.

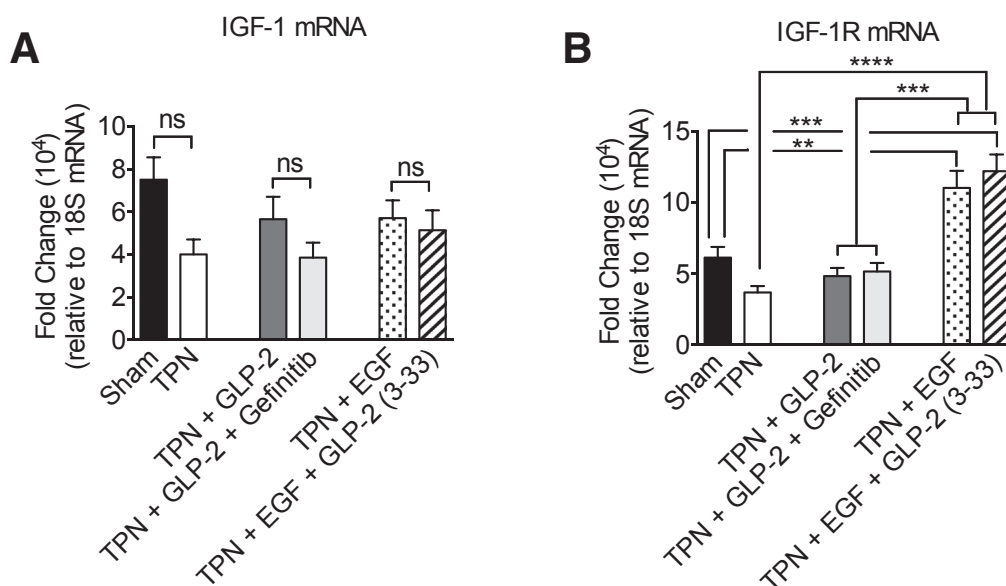
## Discussion

TPN, an essential therapy for patients who cannot tolerate enteral nutrition, is associated with mucosal atrophy, barrier dysfunction, and increased clinical complications including higher rates of septicemia.<sup>2,3,52,53</sup> In addition, a significant decrease in mucosally derived growth factors has been reported in TPN patients and in animal models of TPN.<sup>4,26,36,54,55</sup> Thus, for patients dependent on TPN, a promising strategy to improve intestinal growth and maintain epithelial barrier function has been with the use of exogenous growth factors.<sup>56</sup> GLP-2 and GLP-2 analogues have been used successfully in TPN patients to promote intestinal adaptation, improve small intestinal surface area and absorptive function, and can facilitate withdrawal from parenteral nutrition.<sup>5,6,57</sup> Similarly, EGF has been shown to have considerable benefit for pediatric patients with SBS and necrotizing enterocolitis.<sup>58,59</sup> GLP-2 and EGF also have shown synergistic beneficial responses in a rat model of TPN,<sup>27</sup> however, limited information is available on whether

the biological actions of these 2 growth factors occur through overlapping or distinct signaling pathways in the TPN model.<sup>56</sup>

In the present work, we explored the interactions between EGF and GLP-2 in a mouse TPN model. In WT mice receiving TPN, we found reductions in endogenous EGF and GLP-2 signaling pathways including decreased GLP-2 plasma levels and decreased EGF, EGFR, and GLP2R expression in the intestine. Consistent with previous reports in the mouse TPN model,<sup>4,25</sup> both exogenous EGF and GLP-2 attenuated TPN-induced mucosal atrophy and, in both cases, this was associated with maintenance of specific components from each other's signaling pathway. Reciprocal receptor-inhibitor studies using the EGFR kinase inhibitor gefitinib and the GLP-2 antagonist GLP-2 (3-33) clearly showed strong interdependency for the beneficial effects of each growth factor, which required activation of downstream AKT and  $\beta$ -catenin signaling. At a cellular level, we investigated the requirements for EGFR and PI3K/pAKT signaling in IECs using *IEC-Egfr<sup>KO</sup>* and *IEC-pi3kr1<sup>KO</sup>* mice. We found that the beneficial actions of both growth factors required functional EGFR signaling in IECs. Surprisingly, however, EGF was completely dependent on downstream PI3K/pAKT signaling in IECs, whereas GLP-2 appears to attenuate mucosal atrophy and improve IEC proliferation independently of the PI3K pathway. The sustained nuclear  $\beta$ -catenin signaling observed after GLP-2 treatment in the absence of PI3K signaling suggests that activation of the Wnt/ $\beta$ -catenin pathway by GLP-2 may contribute to the attenuation of mucosal atrophy. Finally, we showed that many of the same features of mucosal atrophy observed in the mouse TPN model are recapitulated in the human ileum upon nutrient deprivation. These findings indicate that further investigations into the interdependency of EGF and GLP-2 signaling pathways, at a cellular level, may yield new insights into strategies to augment intestinal adaptation.

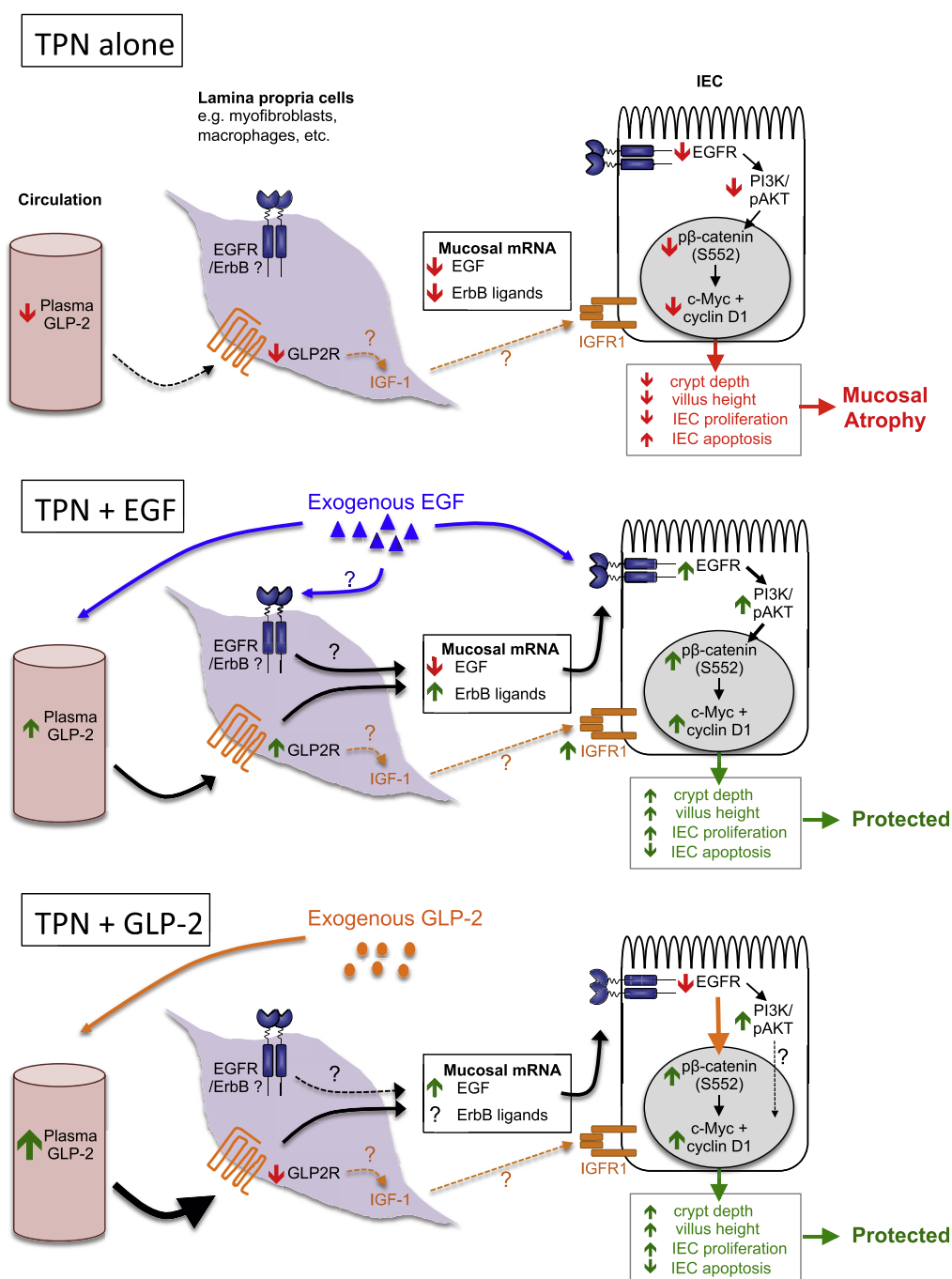
**Figure 11. Mucosal IGF-1 and IGF-1R mRNA expression levels in the mouse TPN model.** IGF-1 and IGF-1R mRNA levels were measured in scraped mucosa from all 6 TPN treatment groups used in this study. (A) Real-time PCR analysis of IGF-1 mRNA expression (n = 5–7 per group). (B) Real-time PCR analysis of IGF-1R mRNA expression in scraped mucosa (n = 5–7 per group). \*\**P* < .01, \*\*\**P* < .001, and \*\*\*\**P* < .0001.





The intestinal stem cell niche contains various accessory cells within the lamina propria such as subepithelial myofibroblasts, enteric neurons, and myeloid cells that provide important, but often redundant, paracrine signals that maintain the crypt stem cell/progenitor compartment. Previous studies have highlighted the importance of ErbB ligand production and EGFR signaling from subepithelial myofibroblasts and myeloid cells for IEC responses during intestinal inflammation and tumorigenesis.<sup>60,61</sup> Although exogenous GLP-2 maintained mucosal EGF expression in the present study, we previously reported that many other ErbB ligands are down-regulated in the mouse TPN model.

For example, down-regulation of neuregulin-4, which specifically binds to ErbB4 receptors, is directly dependent on enhanced TNF $\alpha$  signaling associated with the mild proinflammatory state observed in the mouse TPN model.<sup>19,21</sup> Interestingly, exogenous GLP-2 can acutely induce expression of other ErbB ligands that are required for IEC proliferation in WT mice and after refeeding.<sup>15,16</sup> Likewise, exogenous EGF restored mucosal *Nrg4* mRNA expression in TPN-treated mice.<sup>19</sup> These results indicate that paracrine signaling through other ErbB receptors likely contributes to the beneficial actions of exogenous GLP-2 and EGF in the TPN model. Indeed, in preliminary studies using



IEC-specific *ErbB4*<sup>KO</sup> mice we have observed exacerbated TPN-associated mucosal atrophy.<sup>62</sup> Further studies will be needed to address which accessory cells produce these different ErbB ligands, how their expression is regulated, and whether they act primarily as paracrine growth factors.

In addition to ErbB ligands, other paracrine factors have been implicated in the beneficial actions of GLP-2 in the intestine, including IGF-1. Analysis of *IEC-IGF-1R*<sup>KO</sup> mice showed that IGF-1R and downstream activation of  $\beta$ -catenin signaling in IECs is required for GLP-2 effects on acute IEC proliferation and intestinal adaptation responses.<sup>12,14</sup> Considering that IGF-1R and EGFR/ErbB families show homology in their structure and both the receptors share considerable cross-talk in their functions,<sup>63</sup> it is not surprising that several GLP-2 studies have reported interactions between these 2 growth factor systems in the intestine. Rowland et al<sup>14</sup> reported reduced mucosal Heparin-binding EGF-like growth factor (HB-EGF) and EGFR mRNA levels in *IEC-IGF-1R*<sup>KO</sup> mice. On the other hand, mucosal EGF and IGF-1R mRNA levels were significantly lower in *Glp2r*-deficient mice under basal conditions, whereas EGFR, ErbB ligand epiregulin, and IGF-1 mRNA expression was reduced in re-fed *Glp2r*-deficient mice compared with re-fed WT mice.<sup>15,16</sup> In our own preliminary studies, IGF-1 and IGF-1R mRNA expression levels were unchanged after 6-day TPN administration and were not altered by exogenous GLP-2 treatment. However, exogenous EGF markedly increased IGF-1R mRNA levels independently of GLP2R signaling whereas IGF-1 mRNA levels remained unchanged (Figure 11). Taken together, these findings show complex interactions between GLP2R signaling and paracrine growth factors that activate EGFR and IGF-1R signaling pathways in IECs. Intriguingly, the ability of exogenous GLP-2 to protect against TPN-associated mucosal atrophy independently of intestinal PI3K but still requiring Wnt/ $\beta$ -catenin signaling raises the possibility that intact IGF-1/IGF-1R signaling observed in the mouse TPN model may be involved in this process (Figure 12). Indeed,

accumulating evidence suggests that IGF-1/IGF-1R signaling can activate  $\beta$ -catenin through several different mechanisms including IRS-1-dependent pathways.<sup>64,65</sup> Although beyond the scope of the present work, it will be important to examine the requirement of IGF-1R signaling in IECs for this response and to directly compare GLP-2 actions in both *IEC-Egfr*<sup>KO</sup> and *IEC-Igf-1r*<sup>KO</sup> mice in the mouse TPN model.

Because of continuous cell turnover and high rates of proliferation, the intestinal stem cell (ISC)/progenitor cell populations of the crypt compartment are very metabolically active. Loss of enteral nutrition through long-term caloric depletion, fasting, or parenteral nutrition can alter the function of ISC/progenitor populations as well as that of other accessory cells in the intestinal stem cell niche such as Paneth cells.<sup>66–68</sup> Previous studies have shown that phosphatase and tensin homolog, a negative regulator of the PI3K/AKT/mammalian target of rapamycin complex 1 (mTORC1)-signaling pathway, is an important regulator of reserve facultative ISCs.<sup>67</sup> Upon fasting, the number of rapidly recycling leucine-rich repeat-containing G-protein-coupled receptor 5 (*Lgr5*)+ cells is reduced, but at the same time phosphatase and tensin homolog is selectively inhibited in reserve ISCs making them competent during refeeding to be mobilized and replenish the *Lgr5*+ stem cell pool; a process that is dependent on PI3K/AKT/mTORC1 activation. By contrast, under conditions of long-term caloric restriction, *Lgr5*+ ISC self-renewal is regulated indirectly by decreased mTORC1 signaling in neighboring Paneth cells.<sup>68</sup> In the mouse TPN model, we recently showed that both *Lgr5*+ ISCs and Paneth cell populations are diminished after 6 days of TPN administration. Although the loss of *Lgr5*+ ISCs is consistent with a marked reduction in AKT phosphorylation observed in whole IEC isolates analyzed in this study, it will be important to confirm these findings directly within the crypt stem cell compartment. Because activation of PI3K/pAKT signaling in IECs is essential for the beneficial effects of EGF treatment but not GLP-2 in the TPN model, it raises the possibility that other signaling pathways besides IGF-1/IGF-1R may contribute to

**Figure 12. (See previous page). Summary of the interdependency of EGF and GLP-2 signaling to attenuate mucosal atrophy in a mouse TPN model.** Exogenous EGF and GLP-2 treatment attenuate TPN-associated mucosal atrophy. Based on the results from reciprocal receptor inhibition studies and analyses of IEC responses in *IEC-Egfr*<sup>KO</sup> and *IEC-pi3kr1*<sup>KO</sup> mice, the requirements of EGFR- and PI3K/pAKT-dependent pathways in IECs for the beneficial actions of these 2 growth factors are summarized. *Top panel:* TPN alone. TPN alone reduces components of endogenous EGF and GLP-2 signaling in the intestinal mucosa. Importantly, TPN leads to a reduction in functional EGFR signaling in IECs, decreased cytoplasmic PI3K/pAKT signaling, and decreased p- $\beta$ -catenin (S552), c-Myc, and cyclin D1 levels leading to mucosal atrophy. *Middle panel:* TPN plus exogenous EGF. Exogenous EGF treatment restores GLP-2 plasma levels, mucosal GLP2R expression, and EGFR protein levels in IECs. Exogenous EGF also may enhance the production of ErbB ligands from other lamina propria cells that activate other ErbB receptors on IECs (not shown). The beneficial actions of exogenous EGF are dependent on functional EGFR and PI3K/pAKT signaling in IECs. EGFR/PI3K/pAKT signaling is required for maintenance of nuclear p- $\beta$ -catenin (S552), c-Myc, and cyclin D1 levels needed to improve IEC responses and attenuate mucosal atrophy. *Bottom panel:* TPN plus exogenous GLP-2. Exogenous GLP-2 treatment robustly increases GLP-2 plasma levels and restores mucosal EGF expression. Exogenous GLP-2 also may increase expression of other ErbB ligands in GLP2R-expressing lamina propria cells that activate other ErbB receptors on IECs (not shown). The beneficial actions of exogenous GLP-2 are dependent on functional EGFR signaling in IECs, but GLP-2 still can attenuate mucosal atrophy in the absence of PI3K/pAKT signaling in IECs. Importantly, functional EGFR signaling but not PI3K/pAKT signaling in IECs is required for maintenance of nuclear p- $\beta$ -catenin (S552), c-Myc, and cyclin D1 levels needed to improve IEC responses and attenuate mucosal atrophy. As noted, complex cross-talk between GLP2R and EGFR/ErbB signaling with other signaling pathways such as IGF-1/IGF-1R likely contributes to these beneficial IEC responses. In IECs, IGF-1R signaling also may contribute to activation of Wnt/ $\beta$ -catenin signaling independently of the PI3K/pAKT pathway (see Discussion section for more details).

the actions of GLP-2 in regulating the stem cell niche during enteral nutrient deprivation. Recent ablation studies have shown that Foxl1<sup>+</sup> subepithelial mesenchymal cells provide essential paracrine signals including Wnt ligands for the maintenance of the intestinal stem cell niche.<sup>69</sup> An alternative possibility is that GLP-2 may stimulate Wnt ligand/R-spondin production from accessory cells of the stem cell niche, thereby enhancing Wnt/ $\beta$ -catenin signaling within the crypt compartment. Future work will be needed to test this hypothesis and to further dissect out the contribution of canonical vs noncanonical Wnt pathways for the actions of GLP-2 actions in the mouse TPN model. Consistent with a loss of IEC proliferation observed in healthy volunteers maintained on TPN,<sup>53</sup> we showed a reduction of EGF and GLP-2 signaling components, reduced IEC proliferation, and increased IEC apoptosis in human small bowel not exposed to enteral nutrition, suggesting that a similar effect occurs on a clinical basis. It will be important to determine how these distinct downstream signaling pathways regulate different ISC/progenitor populations after TPN administration and whether the same pathways are required for regulation of the intestinal stem cell niche from patients dependent on TPN.

In summary, we have shown a striking co-dependency of EGF and GLP-2 and their downstream signal transduction pathways in attenuating mucosal atrophy in the mouse model of TPN (summarized in Figure 12). These findings suggest that newer strategies that preserve both of these signals will lead to the most optimal clinical treatment of disorders such as short-bowel syndrome.

## References

- Minard G, Kudsk KA. Nutritional support and infection: does the route matter? *World J Surg* 1998;22:213–219.
- Moore FA, Moore EE, Jones TN, et al. TEN versus TPN following major abdominal trauma—reduced septic morbidity. *J Trauma* 1989;29:916–923.
- Casaer MP, Mesotten D, Hermans G, et al. Early versus late parenteral nutrition in critically ill adults. *N Engl J Med* 2011;365:506–517.
- Demehri FR, Barrett M, Ralls MW, et al. Intestinal epithelial cell apoptosis and loss of barrier function in the setting of altered microbiota with enteral nutrient deprivation. *Front Cell Infect Microbiol* 2013;3:105.
- Sigalet DL, Brindle M, Bector D, et al. A safety and dosing study of glucagon-like peptide 2 in children with intestinal failure. *JPEN J Parenter Enteral Nutr* 2017 Jan 29, pii: S0022-3468(17)30067-2.
- Schwartz LK, O’Keefe SJ, Fujioka K, et al. Long-term teduglutide for the treatment of patients with intestinal failure associated with short bowel syndrome. *Clin Transl Gastroenterol* 2016;7:e142.
- Brubaker PL, Izzo A, Hill M, et al. Intestinal function in mice with small bowel growth induced by glucagon-like peptide-2. *Am J Physiol* 1997;272:E1050–E1058.
- Drucker DJ, Yusta B. Physiology and pharmacology of the enteroendocrine hormone glucagon-like peptide-2. *Annu Rev Physiol* 2014;76:561–583.
- Rowland KJ, Brubaker PL. The “cryptic” mechanism of action of glucagon-like peptide-2. *Am J Physiol Gastrointest Liver Physiol* 2011;301:G1–G8.
- Orskov C, Hartmann B, Poulsen SS, et al. GLP-2 stimulates colonic growth via KGF, released by subepithelial myofibroblasts with GLP-2 receptors. *Regul Pept* 2005;124:105–112.
- Dube PE, Forse CL, Bahrami J, et al. The essential role of insulin-like growth factor-1 in the intestinal tropic effects of glucagon-like peptide-2 in mice. *Gastroenterology* 2006;131:589–605.
- Dube PE, Rowland KJ, Brubaker PL. Glucagon-like peptide-2 activates beta-catenin signaling in the mouse intestinal crypt: role of insulin-like growth factor-I. *Endocrinology* 2008;149:291–301.
- Leen JL, Izzo A, Upadhyay C, et al. Mechanism of action of glucagon-like peptide-2 to increase IGF-I mRNA in intestinal subepithelial fibroblasts. *Endocrinology* 2011;152:436–446.
- Rowland KJ, Trivedi S, Lee D, et al. Loss of glucagon-like peptide-2-induced proliferation following intestinal epithelial insulin-like growth factor-1-receptor deletion. *Gastroenterology* 2011;141:2166–2175 e7.
- Yusta B, Holland D, Koehler JA, et al. ErbB signaling is required for the proliferative actions of GLP-2 in the murine gut. *Gastroenterology* 2009;137:986–996.
- Bahrami J, Yusta B, Drucker DJ. ErbB activity links the glucagon-like peptide-2 receptor to refeeding-induced adaptation in the murine small bowel. *Gastroenterology* 2010;138:2447–2456.
- Hare KJ, Hartmann B, Kissow H, et al. The intestinotrophic peptide, glp-2, counteracts intestinal atrophy in mice induced by the epidermal growth factor receptor inhibitor, gefitinib. *Clin Cancer Res* 2007;13:5170–5175.
- Feng Y, McDunn JE, Teitelbaum DH. Decreased phospho-Akt signaling in a mouse model of total parenteral nutrition: a potential mechanism for the development of intestinal mucosal atrophy. *Am J Physiol Gastrointest Liver Physiol* 2010;298:G833–G841.
- Feng Y, Teitelbaum DH. Epidermal growth factor/TNF- $\alpha$  transactivation modulates epithelial cell proliferation and apoptosis in a mouse model of parenteral nutrition. *Am J Physiol Gastrointest Liver Physiol* 2012;302:G236–G249.
- Feng Y, Teitelbaum DH. Tumour necrosis factor-induced loss of intestinal barrier function requires TNFR1 and TNFR2 signalling in a mouse model of total parenteral nutrition. *J Physiol* 2013;591:3709–3723.
- Feng Y, Tsai YH, Xiao W, et al. Loss of ADAM17-mediated tumor necrosis factor  $\alpha$  signaling in intestinal cells attenuates mucosal atrophy in a mouse model of parenteral nutrition. *Mol Cell Biol* 2015;35:3604–3621.
- Burrin DG, Stoll B, Guan X, et al. Glucagon-like peptide 2 dose-dependently activates intestinal cell survival and proliferation in neonatal piglets. *Endocrinology* 2005;146:22–32.
- Burrin DG, Stoll B, Jiang R, et al. GLP-2 stimulates intestinal growth in premature TPN-fed pigs by suppressing proteolysis and apoptosis. *Am J Physiol Gastrointest Liver Physiol* 2000;279:G1249–G1256.

24. Chance WT, Foley-Nelson T, Thomas I, et al. Prevention of parenteral nutrition-induced gut hypoplasia by coinfusion of glucagon-like peptide-2. *Am J Physiol* 1997; 273:G559–G563.
25. Lei Q, Bi J, Wang X, et al. GLP-2 prevents intestinal mucosal atrophy and improves tissue antioxidant capacity in a mouse model of total parenteral nutrition. *Nutrients* 2016;8:33.
26. Sangild PT, Tappenden KA, Malo C, et al. Glucagon-like peptide 2 stimulates intestinal nutrient absorption in parenterally fed newborn pigs. *J Pediatr Gastroenterol Nutr* 2006;43:160–167.
27. Kitchen PA, Goodlad RA, FitzGerald AJ, et al. Intestinal growth in parenterally-fed rats induced by the combined effects of glucagon-like peptide 2 and epidermal growth factor. *JPEN J Parenter Enteral Nutr* 2005;29:248–254.
28. Suri M, Turner JM, Sigalet DL, et al. Exogenous glucagon-like peptide-2 improves outcomes of intestinal adaptation in a distal-intestinal resection neonatal piglet model of short bowel syndrome. *Pediatr Res* 2014; 76:370–377.
29. el Marjou F, Janssen KP, Chang BH, et al. Tissue-specific and inducible Cre-mediated recombination in the gut epithelium. *Genesis* 2004;39:186–193.
30. Ireland H, Kemp R, Houghton C, et al. Inducible Cre-mediated control of gene expression in the murine gastrointestinal tract: effect of loss of beta-catenin. *Gastroenterology* 2004;126:1236–1246.
31. Lee G, Goretsky T, Managlia E, et al. Phosphoinositide 3-kinase signaling mediates beta-catenin activation in intestinal epithelial stem and progenitor cells in colitis. *Gastroenterology* 2010;139:869–881, e1–9.
32. Lee TC, Threadgill DW. Generation and validation of mice carrying a conditional allele of the epidermal growth factor receptor. *Genesis* 2009;47:85–92.
33. Luo J, McMullen JR, Sobkiw CL, et al. Class IA phosphoinositide 3-kinase regulates heart size and physiological cardiac hypertrophy. *Mol Cell Biol* 2005; 25:9491–9502.
34. Thulesen J, Knudsen LB, Hartmann B, et al. The truncated metabolite GLP-2 (3-33) interacts with the GLP-2 receptor as a partial agonist. *Regul Pept* 2002;103:9–15.
35. Karaman MW, Herrgard S, Treiber DK, et al. A quantitative analysis of kinase inhibitor selectivity. *Nat Biotechnol* 2008;26:127–132.
36. Brinkman AS, Murali SG, Hitt S, et al. Enteral nutrients potentiate glucagon-like peptide-2 action and reduce dependence on parenteral nutrition in a rat model of human intestinal failure. *Am J Physiol Gastrointest Liver Physiol* 2012;303:G610–G622.
37. Brubaker PL, Crivici A, Izzo A, et al. Circulating and tissue forms of the intestinal growth factor, glucagon-like peptide-2. *Endocrinology* 1997;138:4837–4843.
38. Grossmann J, Maxson JM, Whitacre CM, et al. New isolation technique to study apoptosis in human intestinal epithelial cells. *Am J Pathol* 1998;153:53–62.
39. Dekaney CM, Rodriguez JM, Graul MC, et al. Isolation and characterization of a putative intestinal stem cell fraction from mouse jejunum. *Gastroenterology* 2005; 129:1567–1580.
40. Traber PG, Gumucio DL, Wang W. Isolation of intestinal epithelial cells for the study of differential gene expression along the crypt-villus axis. *Am J Physiol* 1991; 260:G895–G903.
41. John LJ, Fromm M, Schulzke JD. Epithelial barriers in intestinal inflammation. *Antioxid Redox Signal* 2011; 15:1255–1270.
42. Salim SY, Soderholm JD. Importance of disrupted intestinal barrier in inflammatory bowel diseases. *Inflamm Bowel Dis* 2011;17:362–381.
43. Shin ED, Estall JL, Izzo A, et al. Mucosal adaptation to enteral nutrients is dependent on the physiologic actions of glucagon-like peptide-2 in mice. *Gastroenterology* 2005;128:1340–1353.
44. Garrison AP, Dekaney CM, von Allmen DC, et al. Early but not late administration of glucagon-like peptide-2 following ileo-cecal resection augments putative intestinal stem cell expansion. *Am J Physiol Gastrointest Liver Physiol* 2009;296:G643–G650.
45. Okawada M, Holst JJ, Teitelbaum DH. Administration of a dipeptidyl peptidase IV inhibitor enhances the intestinal adaptation in a mouse model of short bowel syndrome. *Surgery* 2011;150:217–223.
46. Trivedi S, Wiber SC, El-Zimaity HM, et al. Glucagon-like peptide-2 increases dysplasia in rodent models of colon cancer. *Am J Physiol Gastrointest Liver Physiol* 2012; 302:G840–G849.
47. Yusta B, Estall J, Drucker DJ. Glucagon-like peptide-2 receptor activation engages bad and glycogen synthase kinase-3 in a protein kinase A-dependent manner and prevents apoptosis following inhibition of phosphatidylinositol 3-kinase. *J Biol Chem* 2002; 277:24896–24906.
48. Munroe DG, Gupta AK, Kooshesh F, et al. Prototypic G protein-coupled receptor for the intestinotrophic factor glucagon-like peptide 2. *Proc Natl Acad Sci U S A* 1999; 96:1569–1573.
49. Lim DW, Wales PW, Turner JM, et al. On the horizon: trophic peptide growth factors as therapy for neonatal short bowel syndrome. *Expert Opin Ther Targets* 2016; 20:819–830.
50. Yan F, Cao H, Cover TL, et al. Colon-specific delivery of a probiotic-derived soluble protein ameliorates intestinal inflammation in mice through an EGFR-dependent mechanism. *J Clin Invest* 2011;121:2242–2253.
51. Wildhaber BE, Yang H, Spencer AU, et al. Lack of enteral nutrition—effects on the intestinal immune system. *J Surg Res* 2005;123:8–16.
52. Buzby GP. Overview of randomized clinical trials of total parenteral nutrition for malnourished surgical patients. *World J Surg* 1993;17:173–177.
53. Buchman AL, Moukarzel AA, Bhuta S, et al. Parenteral nutrition is associated with intestinal morphologic and functional changes in humans. *JPEN J Parenter Enteral Nutr* 1995;19:453–460.
54. Hua Z, Turner JM, Sigalet DL, et al. Role of glucagon-like peptide-2 deficiency in neonatal short-bowel syndrome using neonatal piglets. *Pediatr Res* 2013;73:742–749.
55. McAndrew HF, Lloyd DA, Rintala R, et al. The effects of intravenous epidermal growth factor on bacterial



- translocation and central venous catheter infection in the rat total parenteral nutrition model. *Pediatr Surg Int* 2000; 16:169–173.
56. Warner BW. The pathogenesis of resection-associated intestinal adaptation. *Cell Mol Gastroenterol Hepatol* 2016;2:429–438.
  57. Jeppesen PB, Gilroy R, Pertkiewicz M, et al. Randomised placebo-controlled trial of teduglutide in reducing parenteral nutrition and/or intravenous fluid requirements in patients with short bowel syndrome. *Gut* 2011; 60:902–914.
  58. Sigalet DL, Martin GR, Butzner JD, et al. A pilot study of the use of epidermal growth factor in pediatric short bowel syndrome. *J Pediatr Surg* 2005;40:763–768.
  59. Sullivan PB, Lewindon PJ, Cheng C, et al. Intestinal mucosa remodeling by recombinant human epidermal growth factor(1–48) in neonates with severe necrotizing enterocolitis. *J Pediatr Surg* 2007;42:462–469.
  60. Lu N, Wang L, Cao H, et al. Activation of the epidermal growth factor receptor in macrophages regulates cytokine production and experimental colitis. *J Immunol* 2014;192:1013–1023.
  61. Neufert C, Becker C, Tureci O, et al. Tumor fibroblast-derived epiregulin promotes growth of colitis-associated neoplasms through ERK. *J Clin Invest* 2013; 123:1428–1443.
  62. Feng Y, Dempsey PJ, Frey MR, et al. Intestine-specific ErbB4 deficiency exacerbates TPN associated intestinal atrophy. *Gastroenterology* 2014;146, S-301.
  63. Adams TE, McKern NM, Ward CW. Signalling by the type 1 insulin-like growth factor receptor: interplay with the epidermal growth factor receptor. *Growth Factors* 2004; 22:89–95.
  64. Bortvedt SF, Lund PK. Insulin-like growth factor 1: common mediator of multiple enterotrophic hormones and growth factors. *Curr Opin Gastroenterol* 2012; 28:89–98.
  65. Zeller E, Hammer K, Kirschnick M, et al. Mechanisms of RAS/beta-catenin interactions. *Arch Toxicol* 2013; 87:611–632.
  66. Feng Y, Barrett M, Hou Y, et al. Homeostasis alteration within small intestinal mucosa after acute enteral refeeding in total parenteral nutrition mouse model. *Am J Physiol Gastrointest Liver Physiol* 2016;310:G273–G284.
  67. Richmond CA, Shah MS, Deary LT, et al. Dormant intestinal stem cells are regulated by PTEN and nutritional status. *Cell Rep* 2015;13:2403–2411.
  68. Yilmaz OH, Katajisto P, Lamming DW, et al. mTORC1 in the Paneth cell niche couples intestinal stem-cell function to calorie intake. *Nature* 2012;486:490–495.
  69. Aoki R, Shoshkes-Carmel M, Gao N, et al. Foxl1-expressing mesenchymal cells constitute the intestinal stem cell niche. *Cell Mol Gastroenterol Hepatol* 2016;2:175–188.

---

Received September 2, 2016. Accepted December 31, 2016.

#### Correspondence

Address correspondence to: Peter J. Dempsey, PhD, Division of Gastroenterology, Hepatology and Nutrition, Department of Pediatrics, University of Colorado Medical School, Aurora, Colorado 80045. e-mail: [peter.dempsey@ucdenver.edu](mailto:peter.dempsey@ucdenver.edu); fax: (303) 724–6538.

#### Acknowledgments

Yongjia Feng, Peter J. Dempsey, and Daniel H. Teitelbaum conceived the study, designed the experiments, supervised the study, and drafted the manuscript; Yongjia Feng, Farok R. Demehri, Weidong Xiao, Yu-Hwai Tsai, Jennifer C. Jones, Constance D. Brindley, Jens J. Holst, Bolette Hartmann, and Peter J. Dempsey acquired, analyzed, and interpreted the data; David W. Threadgill and Terrence A. Barrett provided material support; Yongjia Feng, Jens J. Holst, Terrence A. Barrett, and Peter J. Dempsey critically revised the manuscript; and Daniel H. Teitelbaum and Peter J. Dempsey provided funding.

#### Conflicts of interest

The authors disclose no conflicts.

#### Funding

This study was supported by National Institutes of Health grants R01-DK093697 (P.J.D.), R01-AI044076 (D.H.T.), and 2R01 DK095662 (T.A.B.).